



Physicochemical and Functional Similarity Assessment Between Proposed Bevacizumab Biosimilar BAT1706 and Reference Bevacizumab

Di Cao¹ · Chunping Deng¹ · Guangying Wang¹ · Xiong Mei¹ · Jianhua Xie¹ · Yuanmei Liu¹ · Yujie Liu¹ · Yili Yang¹ · Shengfeng Li¹ · Cuihua Liu¹

Accepted: 26 June 2023 / Published online: 22 July 2023
© The Author(s) 2023

Abstract

Background BAT1706 is a proposed biosimilar of bevacizumab, a vascular endothelial growth factor A (VEGF-A)-targeting biologic used to treat several different cancers, including metastatic colorectal cancer. A comprehensive physicochemical and functional similarity assessment is a key component of demonstrating biosimilarity between a reference biologic and a proposed biosimilar. Here we report the physicochemical and functional similarity of BAT1706 and reference bevacizumab sourced from both the United States (US-bevacizumab) and the European Union (EU-bevacizumab).

Method A large range of product attributes, including primary and higher order structure, post-translational modifications, purity, stability, and potency, were characterized for BAT1706 and EU/US-bevacizumab using sensitive state-of-the-art analytical techniques. Up to 18 lots of US- and 29 lots of EU-bevacizumab, and 10 unique drug substance lots of BAT1706, were assessed.

Result BAT1706 was shown to have an identical amino acid sequence and an indistinguishable higher-order structure compared with EU/US-bevacizumab. BAT1706 and EU/US-bevacizumab also exhibited similar post-translational modifications, glycan profiles, and charge variants. Potency, assessed using a wide range of bioassays, was also shown to be comparable between BAT1706 and EU/US-bevacizumab, with statistical equivalence demonstrated for VEGF-A binding and neutralizing activity.

Conclusion Overall, this extensive comparability exercise demonstrated BAT1706 to match EU/US-bevacizumab in terms of all physicochemical and functional attributes assessed.

Abbreviations

2H2L	2-Heavy-2-light-chain	C1q	Complement component 1q (the first subcomponent of the C1 complex of the classical pathway of complement activation)
ADCC	Antibody-dependent cell-mediated cytotoxicity	CDC	Complement-dependent cytotoxicity
AUC-SV	Analytical ultracentrifugation sedimentation velocity	CE-SDS	Capillary electrophoresis-sodium dodecyl sulfate
BLI	Bio-Layer Interferometry	CI	Confidence interval
		cIEF	Capillary isoelectric focusing
		DLS	Dynamic light scattering
		DSC	Differential scanning calorimetry
		EC ₅₀	Half maximal effective concentration
		ECL	Electrochemiluminescent
		ELISA	Enzyme-linked immunosorbent assay
		EMA	European Medicines Agency
		ESI-TOF-MS	Electrospray ionization-time of flight-mass spectrometer

Di Cao, Chunping Deng have contributed equally to this work and should be considered co-first authors.

✉ Cuihua Liu
chliu@bio-thera.com

¹ Bio-Thera Solutions, Ltd., Floor 5, Building A6, 11 Kai-Yuan Blvd, Huangpu District, Guangzhou 510530, Guangdong, China

ESI-QToF	Electrospray-ionization quadrupole time-of-flight	rCE-SDS	Reduced capillary electrophoresis-sodium dodecyl sulfate
EU	European Union	RI	Refractive index
Fab	Antigen-binding fragment	RP	Reference product
Fc	Crystallizable fragment	RP-HPLC	Reverse-phase-high-performance liquid chromatography
FcRn	Neonatal Fc receptor	RP-UPLC	Reverse-phase ultra-performance liquid chromatography
FcγR	Fcγ receptor	RGA	Reporter gene assay
FDA	US Food and Drug Administration	RTK	Receptor tyrosine kinase
Flowcam	Micro-flow imaging	SD	Standard deviation
FTIR	Fourier-transform infrared spectroscopy	SEC-HPLC	Size exclusion high-performance liquid chromatography
HC	Heavy chain	SEC-HPLC-MALS	Size exclusion high-performance liquid chromatography with multi-angle light scattering
HCP	Host cell protein	SPR	Surface plasmon resonance
HER2	Human epidermal growth factor receptor 2	T_m	Melting temperature
HIC-HPLC	Hydrophobic interaction chromatography-high-performance liquid chromatography	US	United States
HILIC	Hydrophilic interaction liquid chromatography	UV	Ultraviolet
HPLC	High-performance liquid chromatography	UV-CD	Ultraviolet circular dichroism
HRP	Horseradish peroxidase	VEGF-A	Vascular endothelial growth factor A
HUVEC	Human umbilical vein endothelial cells	VEGFR	Vascular endothelial growth factor receptor
IEC-HPLC	Cation exchange high-performance liquid chromatography	VEGFR-1	Vascular endothelial growth factor receptor 1
IgG1	Immunoglobulin G1	VEGFR-2	Vascular endothelial growth factor receptor 2
K_a	Association constant	VEGFR-3	Vascular endothelial growth factor receptor 3
K_d	Dissociation constant		
K_D	Equilibrium constant		
KDR	Kinase insert domain receptor		
LC	Light chain		
LC-MS/MS	Liquid chromatography with tandem mass spectrometry		
LMW	Low molecular weight		
LO	Light obscuration		
luc	Luciferase		
MMW	Middle molecular weight		
MW	Molecular weight		
NFAT	Nuclear factor of activated T cells		
NT	Not tested		
nrCE-SDS	Non-reduced capillary electrophoresis-sodium dodecyl sulfate		
pI	Isoelectric point		
PK	Pharmacokinetics		
PLGF	Placental growth factor		
ppm	Parts per million		
PTM	Post-translational modifications		

Key Summary Points

A tier-based quality attribute assessment demonstrated that BAT1706 is highly similar to both US-sourced Avastin® (Bevacizumab) and EU-sourced Avastin®.

BAT1706 demonstrated high similarity in critical biological quality attributes, including antigen-binding fragment (Fab)-related biological activities, effector functions such as Fcγ receptor (FcγR) IIIa-F158 binding, and neonatal Fc receptor (FcRn) binding that may affect its half-life.

Higher-order structure, post-translation modifications, and impurities were highly similar between BAT1706 and bevacizumab.

1 Introduction

A biosimilar also referred to as a follow-on biologic is a medicine that shows no clinically meaningful differences from an approved biologic medicine for which the patent has expired. A growing number of biosimilars of complex biologics, such as monoclonal antibodies, have been approved in Europe and the United States (US). It is expected that by promoting market competition, biosimilars will increase patient access to costly biological medicines [1, 2].

Biosimilars must be shown to match their reference biologics in terms of safety, efficacy, and quality, following stringent development pathways laid out by regulatory authorities such as the European Medicines Agency (EMA) and the US Food and Drug Administration (FDA) [3–5]. A step-wise, totality-of-evidence development approach is recommended in the regulatory guidance for the development of biosimilars [4]. Due to the intrinsically heterogeneous properties of biologics produced by living cells and since a cell line and manufacturing process that are unique from those of the reference biologic must be established for each biosimilar, biosimilars and reference medicines will have minor differences in product attributes, which do not impact clinical safety and efficacy. A key element of the biosimilar development process is extensive physicochemical and biological characterization using a range of analytical techniques to demonstrate comparability between the biosimilar and the reference medicine. These physicochemical and *in vitro* biological analyses lay the foundation for preclinical and clinical studies designed to confirm biosimilarity.

Bevacizumab (reference medicine: Avastin®; Genentech) is a recombinant humanized monoclonal immunoglobulin G1 (IgG1) antibody that binds to vascular endothelial growth factor A (VEGF-A) [6]. Bevacizumab prevents the binding of VEGF-A to vascular endothelial growth factor receptors (VEGFRs) on the surface of endothelial cells, inhibiting endothelial cell proliferation and new blood vessel formation, thereby leading to normalization of the tumor vasculature [6]. Bevacizumab was first approved by the FDA in 2004 and then by the EMA in 2005 to treat patients with certain types of cancer where tumor vasculature contributes to tumor growth, including metastatic colorectal cancer [7].

BAT1706 (Bio-Thera/Sandoz) is a proposed bevacizumab biosimilar currently under regulatory review by the FDA and EMA. BAT1706 has already been approved by the Chinese National Medical Products Administration and is marketed in China as Pobevcy® (Bio-Thera).

Here, we present the results of a comprehensive comparability exercise designed to assess the physicochemical

and functional similarity of BAT1706 and European Union (EU)- or US-sourced reference bevacizumab (EU-bevacizumab or US-bevacizumab, respectively) using state-of-the-art analytical techniques. A key focus was to determine whether any differences between BAT1706 and EU/US-bevacizumab could affect clinical performance. This analytical comparability exercise was designed to comply with the US and EU regulatory guidelines for the development of biosimilars.

2 Materials and Methods

Batches of US-licensed and EU-authorized bevacizumab manufactured by Genentech, Inc. (a Roche company), were procured for approximately 6 years. The storage conditions and handling procedures of the EU/US-bevacizumab were according to the manufacturer's instructions. EU/US-bevacizumab were tested as part of the analytical similarity assessment plan. BAT1706 was developed by Bio-Thera to have the same strength and presentation as EU/US-bevacizumab.

BAT1706 drug substance was manufactured inhouse from Chinese hamster ovary (CHO-BAT) working cell bank (WCB) following the established and validated standard antibody production processes using a commercial scale bioreactor. Subsequently, BAT1706 was purified in sequential downstream steps including depth filtration, protein A affinity chromatography, low pH inactivation, and anion-exchange and cation-exchange chromatography and nanofiltration. Upon purification, UF/DF buffer exchange was performed with its formulated bulk drug substance. The final product was finished via standard steps of thawing, sterile filtration, fill-in-finish, capping and visual inspection, labeling and packing. The formulation for BAT1706 contains the same excipients as the EU/US-bevacizumab reference product, which consists of a, a-trehalose dehydrate (60 mg/mL), sodium phosphate, and polysorbate 20 (0.4mg/mL), pH 6.1.

2.1 Intact and Reduced Deglycosylated Mass Analysis

An electrospray ionization time of the flight-mass spectrometer (ESI-TOF-MS, Waters, Vion) was used to determine the molecular masses of intact molecules. The subsequently obtained ion spectra were deconvoluted to develop molecular mass profiles. For the calculation of complete molecular weight (MW), it was assumed that there were no C-terminal lysine residues on the heavy chain (HC) and that all disulfide bonds remained attached.

The ESI-TOF-MS technique was also used to determine the molecular masses of reduced and deglycosylated HC and light chain (LC). This also provided further assurance that the polypeptide compositions were as expected.

Samples were initially treated with PNGase F (NEB, CAS #83534-39-8) to remove N-linked glycans and then with urea to denature them. The disulfides were subsequently reduced with dithiothreitol (DTT, Sigma, CAS #3483-12-3). The samples were introduced to the mass spectrometer via reverse-phase chromatography. A deconvolution of the summed ion spectra was performed to obtain molecular mass profiles, which were compared with theoretical mass profiles.

2.2 Reduced and Non-reduced Peptide Mapping

The enzymatic digestion with trypsin was used to carry out the reduced peptide map analysis of samples. Prior to digestion, the samples were initially treated with DTT (Sigma) for reduction, then with iodoacetamide (IAM, Sigma, CAS #144-48-9) for alkylation, and ultimately with PNGase F (NEB) for N-linked glycan removal. The resulting peptides were separated by reverse-phase ultra-performance liquid chromatography (RP-UPLC, ACQUITY UPLC®, Waters) using an increasing gradient of acetonitrile in water. The eluted peaks were detected by ultraviolet (UV) absorbance (214 nm), and the peptides were identified by an electrospray-ionization quadrupole time-of-flight (ESI-QToF) mass spectrometer (liquid chromatography with tandem mass spectrometry [LC-MS/MS], water, Xevo G2-XS).

Digestion with trypsin (Promega, CAS #9002-07-7) under denaturing but non-reducing conditions was used to carry out the non-reduced peptide map analysis of the samples. The resulting peptides were analyzed by reverse-phase high-performance liquid chromatography (RP-HPLC) using an increasing gradient of acetonitrile (Fisher, MS grade, CAS #75-05-8) in water (CNW, MS grade, CAS #7732-18-5) (UV detection at 214 nm). The peptides produced under reducing and non-reducing conditions were compared in order to identify the peptides containing disulfide bonds. The peptide identity was confirmed using HPLC coupled with an ESI-QToF mass spectrometer (LC-MS/MS, waters, Xevo G2-XS), allowing accurate determination of the molecular mass of each peptide.

2.3 Glycan Mapping

The hydrophilic interaction liquid chromatography (HILIC) and fluorescence detection were used to carry out the glycan map analysis of the N-linked glycans. The treatment with amidase PNGase F (NEB) enabled the release of N-glycans. The reducing termini of the released glycans were then labeled through reductive amination with a fluorescent tag, and the labeled glycans were separated by HILIC. Peak identification was performed using mass spectrometry by coupling the HILIC-HPLC with a QToF mass spectrometer for verification against the expected glycan mass.

2.4 Isoelectric Points

The isoelectric points (pIs) were determined by capillary isoelectric focusing (cIEF) analysis. The cIEF was conducted on a capillary electrophoresis separation instrument that includes a coated capillary (Agilent 7100) for separation. Samples were electrophoresed through a pH gradient produced by an ampholytic solution (Pharmalyte carrier ampholytes, GE, CAS #70852-56-1) until they reached a pH equal to their pI. Samples were then mobilized and detected by UV absorbance (280 nm) as they passed through a detection window in the capillary (μ silFC coated capillary, BioCEart). Linear regression was used to determine the peak pIs of the samples based on four pI marker peaks (BioCEart).

2.5 Higher-Order Structure by Fourier-Transform Infrared Spectroscopy and Ultraviolet Circular Dichroism Spectroscopy

The secondary structure was assessed by Fourier-transform infrared (FTIR, Thermo, Nicolet IS10) spectroscopy and far ultraviolet circular dichroism (UV-CD), Applied Photophysics, Chirascan V100). In FTIR spectroscopy, the spectra of the formulation buffer blank were captured under similar circumstances and eliminated from the spectra of the protein solution. The second derivative spectrum was calculated using a nine-point smoothing of the resulting spectra. Thermo OMNIC software's QC Compare function was used to determine how closely the testing molecule's spectra matched those of the reference molecule. A score of 100% similarity reflects identical spectra.

Protein solutions were diluted to approximately 0.7 mg/mL in the test buffer for far UV-CD measurements using cuvettes with a path length of 1 cm. After being adjusted for protein concentration and buffer contributions, the spectra were presented as CD ellipticity.

The tertiary structure was assessed by near UV-CD spectroscopy. For the near UV-CD measurements utilizing cuvettes having a path length of 1 cm, protein solutions were diluted to roughly 0.7 mg/mL in the test buffer. The spectra were presented as CD ellipticity after being adjusted for protein content and buffer contributions.

2.6 Thermal Stability by Differential Scanning Calorimetry

The temperature variations between the testing sample and buffer cells were continually monitored and calibrated by differential scanning calorimetry (DSC, Malvern, VP-Capillary), which was used to evaluate thermal stability. The unfolding of the protein molecules appeared as an endothermic transition on the DSC thermogram and was characterized by the melting temperature (T_m). The testing solutions

were diluted in formulation buffer to achieve a protein concentration of approximately 0.5 mg/mL.

2.7 Subvisible Particles by Light Obscuration and Micro-Flow Imaging

A HIAC 9703 liquid particle counting system (Beckman, 9703+) with a HRLD 150 sensor was utilized to measure subvisible particles by light obscuration (LO). Particle concentration results were reported as cumulative particle counts per container for 5, 10, and 25 μm size ranges.

Subvisible particles were also assessed by the Flowcam[®] particle imaging system (FlowCam, 8000s), which contains a flow cell and a digital camera. Cumulative particle counts per mL for 5 μm particles were reported. The Flowcam[®] data were further analyzed for the concentration of 5 μm non-spherical particles with an aspect ratio of < 0.85 to quantify product-related particles that were likely proteinaceous and thus had a higher risk of immunogenicity.

2.8 Submicron Particles by Dynamic Light Scattering

Submicron particles were assessed by dynamic light scattering (DLS, Wyatt, mini DAWN TREOS). With the help of a formulation buffer, protein solutions were diluted to a concentration of approximately 1 mg/mL, and triplicate measurements were taken for each test solution.

2.9 Aggregates by Analytical Ultracentrifugation Sedimentation Velocity

Aggregates were assessed by analytical ultracentrifugation sedimentation velocity (AUC-SV, Beckman). With the help of a formulation buffer, product solutions were diluted to approximately 0.5 mg/mL, and the AUC-SV measurements (in triplicate) were taken at 45,000 rpm with absorbance at 280 nm.

2.10 Aggregates by Size Exclusion High-performance Liquid Chromatography with Multi-angle Light Scattering Detection

Aggregates were also assessed by size exclusion high-performance liquid chromatography with multi-angle light scattering (SEC-HPLC-MALS). The SEC-HPLC (Waters, e2695 HPLC) method used employed a MALS detector, a refractive index (RI) detector (Waters, 2414RI), and a UV detector at 280 nm. The product solutions were injected at a load of approximately 250 mg into the system. An RI increment rate of 0.185 mL/g was applied to the computation of molar mass. The molar masses of the monomer and dimer were presented as the results.

2.11 Size Variants by SEC-HPLC, Reduced Capillary Electrophoresis-Sodium Dodecyl Sulfate, and Non-reduced Capillary Electrophoresis-Sodium Dodecyl Sulfate

SEC-HPLC was used to examine native, or undenatured, size variants. The SEC-HPLC measurements were made on a Waters e2695 HPLC system with a Tosoh Bioscience TSK-GEL G3000_{SW} column. Analytes were monitored by UV absorbance (280 nm). The percentage of the total peak area, obtained from the peak area of each species, helped in evaluating the purity.

Denatured protein size variations were separated using capillary electrophoresis-sodium dodecyl sulfate (CE-SDS) in reduced or non-reduced circumstances. For non-reduced conditions, drug product samples were denatured using SDS buffer (BioCEart) at 70 °C for 5 min. For reduced conditions, drug product samples were denatured using β -mercaptoethanol (Sigma, CAS #60-24-2) to reduce the disulfide bonds at 70 °C for 10 min. Following denaturation, samples from both reduced and non-reduced states were injected into a bare, fused silica capillary (BioCEart) and segregated according to the hydrodynamic size produced by the applied electric field, where the migration time of small-sized proteins is conversely linked to the overall size. Analytes were monitored by UV absorbance (240 nm). The percentage of the total peak area, obtained from the corrected peak area of each species, helped in evaluating the purity.

2.12 Charge Variants by Ion Exchange High-performance Liquid Chromatography

Charged isoforms in drug product samples were separated on an ion exchange high-performance liquid chromatography (IEC-HPLC) Pro Pac WCX-10 analytical column (Thermo Fisher). Fractions eluted using a salt gradient were monitored by UV absorbance (280 nm). The percentage of the total peak area, obtained from the peak area of each charged isoform group (acidic, main, and basic peaks), helped in evaluating the purity.

2.13 Binding to VEGF-A by Enzyme-Linked Immunosorbent Assay

A solid-phase enzyme-linked immunosorbent assay (ELISA) was used to determine binding affinity to recombinant human VEGF-A. Recombinant VEGF-A₁₂₁ (Sino Biological, Cat No.: 10008-HNAH), VEGF-A₁₄₅ (MyBioSource, Cat No.: MBS691674), VEGF-A₁₆₅ (Sino Biological, Cat No.: 11066-HNAB), VEGF-A₁₈₉ (R&D systems, Cat No.: 8147-VE-025), and VEGF-A₂₀₆ (MyBioSource, Cat No.: MBS692231) were coated onto the wells of ELISA microtiter plates. The serial dilutions of the reference standard,

control sample, and test sample were added and incubated. Following a wash step, a goat anti-human IgG (Fc [crystallizable fragment]) conjugated to horseradish peroxidase (HRP; Jackson Immuno Research; Cat No.: 109-035-098) was added to detect bound samples. A substrate/chromogen solution was applied to the wells following a final wash. In the presence of HRP, the substrate changed color according to the concentration of bevacizumab bound to VEGF-A. The reaction was stopped with 2.0 M sulfuric acid, and absorbance was measured with a microplate reader (SpectraMax M4, Molecular Devices). After assessing the parallelism of the dose-response curves, the binding activity of the sample relative to the reference standard was determined using a four-parameter logistic model fit by SoftMax Pro Software (Molecular Devices). The findings were presented as percentages of relative binding values.

2.14 Binding to VEGF-A by Surface Plasmon Resonance

The kinetics of binding to recombinant VEGF-A were determined by surface plasmon resonance (SPR) using a Biacore™ T200 (Cytiva) with multiple-cycle kinetics methodology. A carboxy-methylated sensor chip with pre-immobilized Protein A (Cytiva) was used to capture the Fc region of bevacizumab. VEGF-A₁₁₁ (R&D systems, Cat No.: 5336-VE-010), VEGF-A₁₂₁ (Novoprotein, Cat No.: C083), and VEGF-A₁₆₅ (Novoprotein, Cat No.: C744) were tested at varying concentrations. The sensorgrams were double-referenced with a blank concentration and a reference cell, and a 1:1 kinetic analysis was performed to determine VEGF-A kinetic constants and binding affinity.

2.15 Neutralizing Activity to VEGF-A (Human Umbilical Vein Endothelial Cells Proliferation Inhibition Bioassay)

To assess the effect of dose-dependent inhibition, human umbilical vein endothelial cells (HUVEC; Science II) are used in the proliferation inhibition assay, which exhibits VEGFRs such as vascular endothelial growth factor receptor 1 (VEGFR-1), vascular endothelial growth factor receptor 2 (VEGFR-2), and vascular endothelial growth factor receptor 3 (VEGFR-3), along with VEGF co-receptors Neuropilin 1 and 2. HUVEC were incubated with varying concentrations of the reference standard and test samples in the presence of a constant concentration of VEGF-A₁₆₅ (Sino Biological, Cat No.: 11066-HNAB). After a timed incubation, WST-8 chromogen solution (Dojindo, Cat No.: CK04) was added to the plates, and absorbance was measured with a microplate reader (SpectraMax M4, Molecular Devices). After assessing the parallelism of the dose-response curves, the neutralizing activity of the sample relative to the reference standard

was determined using a four-parameter logistic model fit by SoftMax Pro Software (Molecular Devices). The results were presented as percentages of relative potency values.

2.16 Neutralizing Activity to VEGF-A (Nuclear Factor of Activated T Cells-Luciferase Reporter Gene Assay)

This VEGF-A neutralization assay is a bioluminescent cell-based assay that measures VEGF-A stimulation and inhibition of VEGFR-2 (kinase insert domain receptor [KDR]) using luciferase-mediated VEGF-responsive cells. The serial dilutions of the reference standard, control, and test sample were added to the same volume of VEGF-A₁₆₅ (Sino Biological, Cat No.: 11066-HNAB). After the incubation at room temperature, the mixture was transferred to a 96-well plate. KDR/nuclear factor of activated T cells (NFAT)-HEK293 were inoculated in the 96-well plate and incubated at 37 °C in a 5% CO₂ incubator. When VEGF-A₁₆₅ binds to KDR, downstream signaling leads to the activation of NFAT, inducing the expression of luciferase, which was detected by adding Bio-Glo™ Reagent (Promega Corporation, Cat No.: G7940) and quantified with a microplate reader (Molecular Devices). After assessing the parallelism of the dose-response curves, the potency of the test sample relative to the reference standard was determined using a four-parameter logistic model fit by SoftMax Pro Software (Molecular Devices). The results were presented as percentages of relative potency values.

2.17 Inhibition of VEGFR-2 Receptor Tyrosine Kinase Autophosphorylation

HUVEC were incubated with varying concentrations of bevacizumab in the presence of a constant concentration of VEGF-A₁₆₅ (Sino Biological, Cat No.: 11066-HNAB). After the specified incubation period, cells were analyzed using a Phospho-VEGFR-2 (Tyr1054) Assay Whole Cell Lysate Kit (Meso Scale Discovery, Cat No.: K151DJD-2). Briefly, cells were lysed in order to capture VEGFR-2 onto streptavidin-coated Meso Scale Discovery plates using a biotinylated antibody against the extracellular portion of VEGFR-2. A SULFO-TAG labeled anti-phosphotyrosine monoclonal antibody was then added for the detection of tyrosine phosphorylation. The addition of a read buffer, followed by electrical activation of the plate, resulted in an electrochemiluminescent (ECL) signal that was detected by a plate reader. The ECL signal counts from the plate reader were proportional to the VEGFR-2 tyrosine phosphorylation levels. The half maximal effective concentration (EC₅₀) of bevacizumab was obtained using a four-parameter logistic model fit by SoftMax Pro Software (Molecular Devices).

2.18 Specificity to VEGF-A by SPR

SPR was used to assess the specificity of bevacizumab binding to VEGF-A using a Biacore™ T200 (Cytiva) with a single-cycle kinetics technique. A carboxy-methylated sensor chip with pre-immobilized Protein A (Cytiva) was used to capture the Fc region of bevacizumab, aflibercept (positive control, Bayer), and VEGFR3-Fc (Positive control, Sino Biological, Cat No.: 10806-H02H). VEGF-A₁₂₁ (Novoprotein, Cat No.: C744), VEGF-A₁₆₅ (Novoprotein, Cat No.: C083), VEGF-B (ACRO Biosystems, Cat No.: VE6-H5225), VEGF-C (ACRO Biosystems, Cat No.: VEC-H4225), VEGF-D (ACRO Biosystems, Cat No.: VED-H5228), and placental growth factor (PLGF) (ACRO Biosystems, Cat No.: PGF-H5229) were tested at a fixed concentration. In addition, the sensorgrams were double-referenced with a blank concentration and a reference cell, and a 1:1 kinetic analysis was performed to determine binding kinetic constants.

2.19 Binding to Neonatal Fc Receptor, FcγRIIa, FcγRIIb, FcγRIIIb by Bio-Layer Interferometry

Bio-Layer Interferometry (BLI) was used to quantify the binding affinity to neonatal Fc receptor (FcRn), FcRIIa-131H/131R, FcRIIb, and FcRIIIb using an Octet QKe (ForteBio) with multiple-cycle kinetics technique. A sensor chip with pre-immobilized streptavidin (ForteBio, Cat No.: 18-5019) was used to capture the biotinylated human FcRn (ACRO Biosystems, FCM-H82W4), FcγRIIa-131H (ACRO Biosystems, Cat No.: CDA-H82E6), FcγRIIa-131R (ACRO Biosystems, Cat No.: CDA-H82E7), FcγRIIb (ACRO Biosystems, Cat No.: CDB-H82E0), and FcγRIIIb (ACRO Biosystems, Cat No.: CDB-H82Ea). Bevacizumab was tested at different concentrations. Double-referenced sensorgrams were fitted to a steady-state affinity model for the affinity constant.

2.20 Binding to FcγRIa, FcγRIIIa by SPR

SPR was used to measure the binding affinity to FcγRIa and FcγRIIIa-158V/158F utilizing a Biacore™ T200 (Cytiva) with multiple-cycle kinetics methodology. The Fc region of bevacizumab was detected using a carboxy-methylated sensor chip with pre-immobilized Protein A (Cytiva). FcγRIa (ACRO Biosystems, Cat No.: FCA-H52H1) and FcγRIIIa-158V (ACRO Biosystems, Cat No.: CDA-H82E8), FcγRIIIa-158F (ACRO Biosystems, Cat No.: CD8-H82E9) were tested at different concentrations. Double-referenced sensorgrams were fitted to a 1:1 kinetic or steady-state affinity model for the affinity constant.

2.21 Binding to Complement Component 1q by BLI

BLI was used to quantify the binding affinity to complement component 1q (C1q) by using an Octet QKe (ForteBio) with multiple-cycle kinetics methodology. The LC of bevacizumab was captured using a sensor chip with pre-immobilized Protein L (ForteBio, Cat No.: 18-5085). C1q (Quidel, Cat No.: A400) was tested at different concentrations. Double-referenced sensorgrams were fitted to a steady-state affinity model for the affinity constant.

2.22 Antibody-Dependent Cell-Mediated Cytotoxicity

Antibody-dependent cell-mediated cytotoxicity (ADCC) activity of bevacizumab was evaluated by a bioluminescent cell-based reporter gene assay. NFAT-FcγRIIIa (158V) Jurkat cells, which stably express FcγRIIIa (158V) and NFAT luciferase, were used as effector cells. DLD-1 cells (adenocarcinoma cells), Calu-6 cells (lung epithelial carcinoma cells) that secrete VEGF-A, and SKOV-3 cells (human ovarian carcinoma cells) that express both the secreted and cell-surface associated isoforms of VEGF-A were used as target cell lines. Besides, CD20 expressing cell lines, Raji, and an anti-CD20 monoclonal antibody (Ofatumumab, Novartis) were used as positive controls while adalimumab (AbbVie) was utilized as a negative control in the ADCC assay using DLD-1 and Calu-6 cells. Furthermore, an anti-human epidermal growth factor receptor 2 (HER2) monoclonal antibody (trastuzumab, Roche), which binds to the HER2 expressed on SKOV-3 cells, was used as a positive control, whereas adalimumab was used as a negative control in the ADCC assay using SKOV-3 cells. In the ADCC assay, target cells and NFAT-FcγRIIIa (158V) Jurkat cells were inoculated in a 96-well plate and incubated with a serial dilution of bevacizumab samples or controls. After a specified incubation period in a 5% CO₂ incubator at 37 °C, cell cytotoxicity was detected by adding ONE-Glo™ Luciferase Assay Reagent (Promega, Cat No.: E6120) and quantitated with a Multi-Mode reader (SpectraMax M4, Molecular Devices).

2.23 Complement-Dependent Cytotoxicity

To evaluate complement-dependent cytotoxicity (CDC) activity, three target cell lines were used, which include DLD-1 cells (adenocarcinoma cells), Calu-6 cells (lung epithelial carcinoma cells) that secrete VEGF-A, and SKOV-3 cells (human ovarian carcinoma cells) that express both the secreted and cell-surface associated isoforms of VEGF-A. Moreover, in the case of positive controls for the CDC assay, CD20 expressing cell lines, Raji, and ofatumumab were used, while adalimumab was utilized as a negative control. Target cells were incubated with different dose

concentrations of bevacizumab or control followed by the addition of human complement (Quidel, Cat No.: A112). After a specified incubation period in a 5% CO₂ incubator at 37 °C, CDC activity was monitored by determining cell viability by reading the absorbance at 450 nm (OD450) with WST-8 reagent (Dojindo, Cat No.: CK04).

2.24 Stability and Degradation at Accelerated/Stressed Conditions

The thermal stability and degradation profiles of BAT1706 drug product and reference bevacizumab were determined at 25, 40, and 50 °C, low pH, light exposure, oxidation, vibration, and freeze-thaw cycles. The degradation samples were then characterized using SEC-HPLC, reduced capillary electrophoresis-sodium dodecyl sulfate (rCE-SDS), IEC-HPLC, potency assays, and post-translational modifications (PTMs).

2.25 Protein Concentration

The protein concentration in the solution was determined by UV absorbance using the product extinction coefficient (1.7).

2.26 Volume

The analytical procedure for volume determination complied with PhEur 2.9.17.

3 Results

The attributes assessed for BAT1706 and EU/US-bevacizumab, along with the analytical techniques used, are shown in Table 1. Where applicable, orthogonal methods were used to analyze product attributes and activities comprehensively.

Up to 18 batches of US-bevacizumab and 29 batches of EU-bevacizumab were tested over 6 years. The BAT1706 batches utilized in similarity assessments represent drug product lots formed from 10 different drug substance lots. At least 10 lots of BAT1706 were tested for product attributes that could be affected by the drug substance upstream manufacturing process, e.g., glycan compositions and purity. Different drug product batches developed from the same drug substance lots were also examined for similarity in product attributes that could be altered by fill-and-finish procedures, such as volume and concentration. This testing strategy resulted in a large number of datasets, which enabled meaningful comparisons, including the use of statistical analysis per regulatory agency guidelines. The data from this comparability exercise was evaluated using the statistical analysis approach recommended by the FDA in its recent draft guideline [5]. In this risk-based approach,

the quality attributes of the products are ranked according to their potential risk of clinical impact, in a tiering system, as shown in Table 2.

3.1 Primary Structure and PTMs

Analytical tools were used to investigate the primary structures, glycosylation patterns, and PTMs of BAT1706 and EU/US-bevacizumab. These tools included, but were not limited to, high-resolution and accurate mass spectrometry of protein sequences and HILIC-HPLC-fluorescence for sensitive detection of oligosaccharide profiles. As shown in Fig. 1A, the major components of the antibody were all attached to two core fucosylated glycan isoforms with 0, 1, or 2 terminal galactose residues, referred to as G0F, G1F, and G2F, respectively. These peaks were characterized as the major glycans and the glycosylation pattern of the major glycans was comparable between BAT1706 and EU/US-bevacizumab. In terms of low-abundant glycan structures, small differences were observed between BAT1706 and EU/US-bevacizumab, including glycan forms that had only one HC connected to the glycan chain (labeled in Fig. 1A as G0F/unoccupied), which were only present in EU/US-bevacizumab. The intact molecular masses of all major species were compatible with the products' theoretical masses (Table 2).

The molecular mass results after deglycosylation further demonstrated the highly similar MWs of the HC and LC peptides of BAT1706 and EU/US-bevacizumab (Table 2). In the case of HC peptides, the molecular masses after deglycosylation ranged from 49,711.8 to 49,712.0 Da for BAT1706, 49,711.9 to 49,712.0 Da for US-bevacizumab, and 49,711.9-49,712.0 Da for EU-bevacizumab. In the case of LC peptides, the molecular masses after deglycosylation ranged from 23,446.7-23,446.8 Da, 23,446.7-23,446.9 Da, and 23,446.7-23,446.8 Da, respectively.

An ion signal chromatography overlay (Fig. 1C) was used to compare the peptide mapping between BAT1706 and EU/US-bevacizumab. The peptide mapping analysis confirmed that the primary structures were identical, with 100% of sequence coverage.

PTMs are a significant source of variability in antibody products and were found in both BAT1706 and EU/US-bevacizumab. A single N-linked glycosylation site on the HC located at Asn303 was detected in all BAT1706 and EU/US-bevacizumab peptide maps. Liquid chromatography with mass spectrometry (LC-MS) analysis of the glycopeptides revealed that the prevalent glycan structure was a fucosylated biantennary complex structure with a terminal galactose of 0 or 1, consistent with the glycan mapping results.

Several post-translationally modified peptide segments of lower abundance were observed in both BAT1706 and EU/US-bevacizumab. These included cyclization of the

Table 1 Analytical techniques used for the physicochemical and functional characterization of BAT1706 and EU/US-bevacizumab

Category	Analytical technique
Primary structure, glycosylation and post-translational modifications	Molecular mass of intact whole protein Molecular mass of reduced and deglycosylated HC and LC Protein sequence by reduced peptide map Disulfide structure by non-reduced peptide map N-glycan map by HILIC HPLC Extinction coefficient by Edelhoch method
Higher order structure	Secondary structure by FTIR Tertiary structure by near UV-CD Thermal stability by DSC
Particles and aggregates	Subvisible particles by light obscuration Subvisible particles by MFI Submicron particle profile by DLS Aggregates by AUC-SV Aggregates by SEC-HPLC-MALS
Product-related substances and impurities	Size variants by SEC-HPLC, rCE-SDS, and nrCE-SDS Charge variants by IEC-HPLC Isoelectric point by cIEF
Fab-related biological activities	VEGF-A _{165/121/189} binding by ELISA VEGF-A _{165/121} binding kinetics and affinity by SPR VEGF-A neutralization assay by NFAT-luc reporter gene Proliferation inhibition bioassay by HUVEC cell-based assay
Fc-related biological activities	C1q/FcRn/FcγRIIa (131H)/FcγRIIa (131R)/FcγRIIb/FcγRIIb binding by BLI FcγRIa / FcγRIIIa (158V) / FcγRIIIa (158F) binding by SPR
ADCC/CDC	DLD-1, Calu-6, SK-OV-3
Thermal forced degradation	Thermal stability at 25, 40, and 50°C assessed by purity and potency
General properties	Protein concentration and volume Osmolality, pH, appearance, color, and clarity
Process-related impurities	HCP by ELISA

ADCC antibody-dependent cell-mediated cytotoxicity, *AUC-SV* analytical ultracentrifugation sedimentation velocity, *BLI* Bio-Layer Interferometry, *C1q* the first subcomponent of the C1 complex of the classical pathway of complement activation, *CDC* complement-dependent cytotoxicity, *cIEF* capillary isoelectric focusing, *DLS* dynamic light scattering, *DSC* differential scanning calorimetry, *ELISA* enzyme-linked immunosorbent assay, *Fab* antigen-binding fragment, *FcRn* neonatal Fc receptor, *FcγR* Fcγ receptor, *FTIR* Fourier-transform infrared spectroscopy, *HC* heavy chain, *HCP* host cell protein, *HILIC* hydrophilic interaction liquid chromatography, *HPLC* high-performance liquid chromatography, *HUVEC* human umbilical vein endothelial cells, *IEC-HPLC* cation exchange high-performance liquid chromatography, *LC* light chain, *luc* luciferase, *NFAT* nuclear factor of activated T cells, *nrCE-SDS* non-reduced capillary electrophoresis-sodium dodecyl sulfate, *rCE-SDS* reduced capillary electrophoresis-sodium dodecyl sulfate, *SEC-HPLC* size exclusion high-performance liquid chromatography, *SEC-HPLC-MALS* size exclusion high-performance liquid chromatography with light scattering, *SPR* surface plasmon resonance, *UV-CD* ultraviolet circular dichroism, *VEGF-A* vascular endothelial growth factor A

HC N-terminal Glu residue to pyroglutamate, truncation of the HC C-terminal Lys453 residue, and some deamidation and oxidation sites. Overall, the same PTM sites and similar PTM levels were observed in both BAT1706 and EU/US-bevacizumab.

Both BAT1706 and EU/US-bevacizumab were shown to contain 32 cysteine residues. Non-reduced peptide mapping was performed to map the disulfide bridging patterns. As shown in Fig. 1D, these residues formed a total of 16 disulfide bridges, including 12 intra- and four inter-chain disulfide bridges. The number and position of the disulfide bridges were the same in both BAT1706 and EU/US-bevacizumab.

3.2 Glycosylation

From the visual comparison, BAT1706 and EU/US-bevacizumab have similar oligosaccharide profile patterns assessed by HILIC-UPLC, as shown in Fig. 2A. The glycan forms that could be identified by mass spectrometry are labeled in Fig. 2B. The same oligosaccharide species were present in both BAT1706 and EU/US-bevacizumab. Based on the potential impact of the polysaccharide on pharmacokinetics (PK) or biological function, we classified the oligosaccharides into four broad categories: high mannose, afucosylation, galactosylation, and sialylation. The abundance of each of these oligosaccharide

Table 2 Summary of attributes assessed for BAT1706 and EU/US-bevacizumab.

Tier	Classification	Methods used to compare BAT1706 and EU/US-bevacizumab (RP)		
1	Most clinically relevant attributes	Equivalence test Equivalence between BAT1706 and RP is shown if the calculated 90% two-sided confidence interval of the difference in mean activity between BAT1706 and RP is within ± 1.5 SD		
2	Attributes not directly related to clinical activity Attributes of high abundance that can be quantified	Quality range Greater than 90% of BAT1706 lots must fall within the range of $RP_{\text{mean}} \pm 3SD_{\text{RP}}$		
3	Attributes at low risk of being related to clinical activity Attributes of low abundance Attributes qualitatively assessed Orthogonal method to the Tier 2 method	Predefined limit Characterization result falls into the method variation range Visual comparison Qualitative comparisons of chromatograms or data scatter plots		
Attribute	Tier	BAT1706, Range (n)	US-bevacizumab, Range (n)	EU-bevacizumab, Range (n)
Intact molecular weight (Da) Glycosylation—G0F:G0F	3	146,312.1–146,312.4 (4)	146,311.5–146,311.9 (4)	146,312.0–146,312.3 (4)
Deglycosylated intact molecular weight (Da)	3	149,201.2–149,201.8 (4)	149,201.2–149,201.9(4)	149,201.2–149,201.9 (4)
Reduced and deglycosylated heavy chain (Da)	3	49,711.8–49,712.0 (4)	49,711.9–49,712.0 (4)	49,711.9–49,712.0 (4)
Reduced and deglycosylated light chain (Da)	3	23,446.7–23,446.8 (4)	23,446.7–23,446.9 (4)	23,446.7–23,446.8 (4)
Glycosylation at ASN303 (%)	3	100 (3)	97.7–98.2 (3)	98.2–98.4 (3)
Oxidation at MET258 (%)	3	1.3–2.3 (4)	1.5–2.1 (3)	1.6–2.0 (3)
Glycan map (%)				
High mannose	2	0.7–1.1 (10)	0.5–1.7 (17)	0.5–0.8 (29)
Afucosylation	2	3.4–5.1 (10)	1.6–2.5 (17)	1.6–2.3 (29)
Galactosylation	2	19.5–28.9 (10)	6.3–14.7 (17)	7.2–20.4 (29)
Sialylation	2	1.0–1.4 (10)	0.1–0.3 (17)	0.1–0.5 (29)
FTIR/spectral similarity	3	Visually similar (3)	Visually similar (3)	Visually similar (3)
Near UV-CD/spectral similarity	3	Visually similar (3)	Visually similar (3)	Visually similar (3)
DSC (C) profile	3	Visually similar (5)	Visually similar (3)	Visually similar (3)
T_{m1} (°C)	3	72.8–73.0 (5)	73.0–72.9 (3)	72.9–72.9 (3)
T_{m2} (°C)	3	84.1–84.1 (5)	84.1–84.2 (3)	84.0–84.3 (3)
LO subvisible particle (particles/container)				
$\geq 5 \mu\text{m}$	3	140–1310 (5)	NT	60–490 (5)
$\geq 10 \mu\text{m}$	3	10–50 (5)	NT	0–10 (5)
$\geq 25 \mu\text{m}$	3	0 (5)	NT	0 (5)
Flowcam® subvisible particle (particles/mL)				
$\geq 5 \mu\text{m}$ non-spherical particles	3	370–1301 (5)	505–572 (3)	112–1167 (3)
$\geq 5 \mu\text{m}$ spherical particles	3	90–931 (5)	101–158 (3)	23–404 (3)
DLS radius (nm)	3	7.5–7.6 (3)	7.0–7.7 (3)	7.3–7.5 (3)
AUC-SV profile	3	Visually similar (3)	Visually similar (3)	Visually similar (3)
SEC-HPLC-MALS MW (kDa)				
Monomer	3	147–148 (3)	148–149 (3)	148–149 (3)
Dimer	3	299–304 (3)	306–314 (3)	323–336 (3)
SEC-HPLC (%)				
Monomer	2	96.0–97.0 (10)	96.0–96.9 (17)	96.1–97.4 (29)
Aggregate	2	3.0–3.9 (10)	3.0–4.0 (17)	2.3–3.7 (29)
IEC-HPLC (%)				
Acidic area	2	19.8–27.5 (10)	24.5–31.0 (17)	25.7–29.4 (29)
Main peak	2	62.8–70.1 (10)	60.9–68.0 (17)	62.7–67.5 (29)
Basic area	2	9.3–10.2 (10)	5.2–9.5 (17)	6.5–8.4 (29)
pI of main peak (cIEF)	3	7.7 (5)	7.7 (3)	7.7 (3)
nrCE-SDS 2H2L (%)	2	96.0–97.4 (10)	96.4–98.5 (14)	96.6–97.9 (29)
nrCE-SDS pre-peaks (%)	2	2.6–3.6 (10)	1.6–3.6 (14)	2.1–3.3 (29)
rCE-SDS HC+LC (%)	2	97.7–98.7 (10)	96.3–97.2 (14)	96.1–97.0 (29)
rCE-SDS LMW+MMW (%)	2	0.8–1.8 (10)	0.9–1.7 (14)	1.2–2.1 (29)

Table 2 (continued)

Attribute	Tier	BAT1706, Range (n)	US-bevacizumab, Range (n)	EU-bevacizumab, Range (n)
Fab-mediated activities by ELISA (relative binding activity [EC ₅₀])				
Binding to VEGF-A ₁₆₅	1	90–111 (12)	90–110 (16)	85–113 (18)
Binding to VEGF-A ₁₂₁	2	88–110 (12)	85–114 (7)	85–105 (7)
Binding to VEGF-A ₁₈₉	3	92–95 (3)	94–107 (3)	89–99 (3)
Binding kinetics to VEGF-A ₁₆₅ by SPR				
On rates K_a (1/Ms)	3	0.94×10^6 – 1.09×10^6 (5)	1.05×10^6 – 1.06×10^6 (3)	1.14×10^6 – 1.29×10^6 (3)
Off rates K_d (1/s)	3	5.47×10^{-5} – 6.01×10^{-5} (5)	3.34×10^{-5} – 3.85×10^{-5} (3)	4.94×10^{-5} – 6.38×10^{-5} (3)
Equilibrium constant K_D (M)	3	5.06×10^{-11} – 6.39×10^{-11} (5)	3.17×10^{-11} – 3.65×10^{-11} (3)	4.31×10^{-11} – 4.93×10^{-11} (3)
Binding kinetics to VEGF-A ₁₂₁ by SPR				
On rates K_a (1/Ms)	3	1.58×10^5 – 1.88×10^5 (5)	1.47×10^5 – 1.56×10^5 (3)	1.46×10^5 – 1.52×10^5 (3)
Off rates K_d (1/s)	3	5.58×10^{-5} – 6.70×10^{-5} (5)	5.90×10^{-5} – 6.30×10^{-5} (3)	6.22×10^{-5} – 6.43×10^{-5} (3)
Equilibrium constant K_D (M)	3	3.11×10^{-11} – 4.09×10^{-11} (5)	3.78×10^{-11} – 4.25×10^{-11} (3)	4.18×10^{-11} – 4.43×10^{-11} (3)
VEGF-A neutralization assay (NFAT-luc reporter gene assay) Relative activity (EC ₅₀)	1	84–107 (12)	78–112 (17)	77–115 (29)
Proliferation inhibition bioassay (HUVEC) relative activity (EC ₅₀)	1	85–109 (12)	83–113 (18)	84–116 (29)
Inhibition of VEGFR-2 RTK Autophosphorylation (EC ₅₀)	3	175–225 ng/mL (4)	178–227 ng/mL (3)	175–229 ng/mL (3)
Specificity to VEGF-A by SPR Binding specificity to VEGF-A isoforms	3	VEGF-A specific (1)	VEGF-A specific (1)	VEGF-A specific (1)
Fc binding affinity, K_D (M)				
C1q binding (by BLI)	2	4.66×10^{-9} – 6.77×10^{-9} (12)	6.27×10^{-9} – 9.77×10^{-9} (13)	5.19×10^{-9} – 8.78×10^{-9} (16)
FcRn binding (by BLI)	2	8.64×10^{-9} – 2.36×10^{-8} (12)	1.78×10^{-8} – 2.99×10^{-8} (13)	1.20×10^{-8} – 2.58×10^{-8} (18)
FcγRIa binding (by SPR)	3	5.39×10^{-11} – 6.20×10^{-11} (5)	5.46×10^{-11} – 6.50×10^{-11} (3)	5.48×10^{-11} – 6.32×10^{-11} (3)
FcγRIIa (131H) binding (by BLI)	3	6.3×10^{-7} – 8.0×10^{-7} (5)	8.4×10^{-7} – 9.0×10^{-7} (3)	7.1×10^{-7} – 8.3×10^{-7} (3)
FcγRIIa (131R) binding (by BLI)	3	7.1×10^{-7} – 8.8×10^{-7} (5)	9.3×10^{-7} – 9.7×10^{-7} (3)	8.1×10^{-7} – 9.3×10^{-7} (3)
FcγRIIb binding (by BLI)	3	1.2×10^{-6} – 1.7×10^{-6} (5)	1.6×10^{-6} – 1.9×10^{-6} (3)	1.3×10^{-6} – 1.5×10^{-6} (3)
FcγRIIIa (158V) binding (by SPR)	2	2.26×10^{-7} – 4.02×10^{-7} (12)	3.26×10^{-7} – 4.23×10^{-7} (10)	3.55×10^{-7} – 4.75×10^{-7} (11)
FcγRIIIa (158F) binding (by SPR)	2	6.94×10^{-7} – 1.06×10^{-6} (12)	7.36×10^{-7} – 1.16×10^{-6} (10)	7.67×10^{-7} – 1.17×10^{-6} (11)
FcγRIIIb binding (by BLI)	3	4.0×10^{-6} – 7.1×10^{-6} (5)	5.5×10^{-6} – 5.9×10^{-6} (3)	5.3×10^{-6} – 6.9×10^{-6} (3)
Fab and Fc-mediated characterization				
Lack of ADCC activity in DLD-1 cells	3	Lack of ADCC (2)	Lack of ADCC (1)	Lack of ADCC (1)
Lack of ADCC activity in Calu-6 cells	3	Lack of ADCC (2)	Lack of ADCC (1)	Lack of ADCC (1)
Lack of ADCC activity in SKOV-3 cells	3	Lack of ADCC (2)	Lack of ADCC (1)	Lack of ADCC (1)
Lack of CDC activity in DLD-1 cells	3	Lack of CDC (2)	Lack of CDC (1)	Lack of CDC (1)
Lack of CDC activity in Calu-6 cells	3	Lack of CDC (2)	Lack of CDC (1)	Lack of CDC (1)
Lack of CDC activity in SKOV3 cells	3	Lack of CDC (2)	Lack of CDC (1)	Lack of CDC (1)
Protein concentration (mg/mL)	2	24.2–26.6 (14)	23.4–25.2(18)	23.7–25.4 (29)
Volume (mL) 100 mg/4 mL	3	4.1–4.2 (6)	NT	4.4–4.5(4)
Volume (mL) 400 mg/16 mL	3	16.3–16.8 (4)	NT	NT
Host cell protein by ELISA (ppm)	3	10–20 (12)	0.2–0.9 (6)	0.3–0.6 (5)

Data presented in the table are the range of minimum to maximum values

n number of batches

2H2L 2-heavy-2-light-chain, *ADCC* antibody-dependent cell-mediated cytotoxicity, *AUC-SV* analytical ultracentrifugation sedimentation velocity, *BLI* Bio-Layer Interferometry, *C1q* the first subcomponent of the C1 complex of the classical pathway of complement activation, *CDC* complement-dependent cytotoxicity, *cIEF* capillary isoelectric focusing, *DLS* dynamic light scattering, *DSC* differential scanning calorimetry, *EC₅₀* half maximal effective concentration, *ELISA* enzyme-linked immunosorbent assay, *Fab* antigen-binding fragment, *Fc* crystallizable fragment, *FcRn* neonatal Fc receptor, *FcγR* Fcγ receptor, *Flowcam* micro-flow imaging, *FTIR* Fourier-transform infrared spectroscopy, *HC* heavy chain, *HUVEC* human umbilical vein endothelial cells, *IEC-HPLC* cation exchange high-performance liquid chromatography, K_a association constant, K_d dissociation constant, K_D equilibrium constant, *LC* light chain, *LMW* low molecular weight, *LO* light obscuration, *luc* luciferase, *MMW* middle molecular weight, *MW* molecular weight, *NFAT* nuclear factor of activated T cells, *NT* not tested, *nrCE-SDS* non-reduced capillary electrophoresis-sodium dodecyl sulfate, ppm, parts per million, *rCE-SDS* reduced capillary electrophoresis-sodium dodecyl sulfate, *RP* reference product, *RTK* receptor tyrosine kinase, *SD* standard deviation, *SEC-HPLC* size exclusion high-performance liquid chromatography, *SEC-HPLC-MALS* size exclusion high-performance liquid chromatography with light scattering, *SPR* surface plasmon resonance, T_m melting temperature, *UV-CD* ultraviolet circular dichroism, *VEGF-A* vascular endothelial growth factor A, *VEGFR-2* vascular endothelial growth factor receptor 2

categories is shown in Table 2. There were some minor differences in oligosaccharide abundances between BAT1706 and EU/US-bevacizumab, but these differences had no effect on biological activities. Each of these oligosaccharide categories is discussed in detail in the following paragraphs.

High mannose Man5, Man6, Man7, and Man8 (Man8') are classified as high mannose glycan forms that have the potential to interact with mannose-binding receptors and lead to accelerated clearance of antibody, potentially impacting PK [8]. When compared to EU/US-bevacizumab, BAT1706 had a very similar amount of high mannose glycan forms (Table 2). These levels ranged from 0.7–1.1% for BAT1706, 0.5–1.7% for US-bevacizumab, and 0.5–0.8% for EU-bevacizumab.

Afucosylation The N-linked glycans lacking core fucose were classified as afucosylated glycan forms and include G0, G1, G1', and G2. The lack of fucose is known to significantly enhance the binding of IgG1 to FcγRIIIa [9]. BAT1706 has a slightly higher level of afucosylation versus EU/US-bevacizumab (ranged from 3.4–5.1% for BAT1706, 1.6–2.5% for US-bevacizumab, and 1.6–2.3% for EU-bevacizumab; Table 2), but the differences were insignificant in terms of FcRIIIa binding activity. Since BAT1706 and EU/US-bevacizumab do not show ADCC activity [10], these differences were considered to be clinically insignificant.

Galactosylation All complex polysaccharide structures containing at least one terminal galactose are classified as galactosylated glycans [11]. Galactosylation may influence C1q binding, which is required for the activation of IgG1-mediated cytotoxicity via CDC [12, 13]. BAT1706 has slightly higher levels of galactosylation than EU/US-bevacizumab (ranged from 19.5–28.9% for BAT1706, 6.3–14.7% for US-bevacizumab, and 7.2–20.4% for EU-bevacizumab; Table 2), but these small differences did not affect C1q-binding activity. Moreover, since VEGF is a soluble antigen, BAT1706 does not exhibit ADCC and CDC effects, hence these small variations in galactosylation levels between BAT1706 and EU/US-bevacizumab were deemed clinically insignificant.

Sialylation Glycan-containing terminal sialic acids are classified as sialylated glycan forms [14]. Both BAT1706 and EU/US-bevacizumab were shown to have low levels of sialylation (ranged from 1.0–1.4% for BAT1706, 0.1–0.3% for US-bevacizumab, and 0.1–0.5% for EU-bevacizumab; Table 2), which have no bioactive or clinically significant effects.

3.3 Higher Order Structure

Results of the analysis of the secondary structure by both far UV-CD and FTIR, and of the tertiary structure by near UV-CD, are shown in Fig. 3A–C, respectively.

The far and near UV-CD profiles were visually similar between BAT1706 and EU/US-bevacizumab (Fig. 3A, B), indicating that their secondary and tertiary structures are identical.

Similarly, the FTIR spectra of BAT1706 and EU/US-bevacizumab showed nearly identical peak positions and intensities (Fig. 3C), indicating the presence of anti-parallel β -sheet structures common in antibodies. Therefore, the CD and FTIR findings show that BAT1706 and EU/US-bevacizumab have identical secondary and tertiary structures.

Furthermore, thermal stability was analyzed by DSC. EU/US-bevacizumab and BAT1706's DSC curves were notably similar to one another visually (Fig. 3D). For EU/US-bevacizumab, the DSC curves showed two thermal transition points corresponding to the structural changes of the antigen-binding fragment (Fab) CH₂ and CH₃ domains, characterized by two thermals T_m (Table 2). The similar T_{m1} and T_{m2} values for BAT1706 and EU/US-bevacizumab further indicate their similar thermal stability (T_{m1} : ranged from 72.8–73.0 °C for BAT1706, 73.0–72.9 °C for US-bevacizumab, and 72.9–72.9 °C for EU-bevacizumab; T_{m2} : ranged from 84.1 to 84.1 °C for BAT1706, 84.1–84.2 °C for US-bevacizumab, and 84.0–84.3 °C for EU-bevacizumab; Table 2).

3.4 Particles and Aggregates

Levels of the subvisible particle in BAT1706 and EU/US-bevacizumab were measured by both LO and Flowcam® methods. The results from each method indicated that the levels of subvisible particles were generally low and similar between BAT1706 and EU/US-bevacizumab (Table 2). As per LO method, the cumulative particle counts per container for $\geq 5 \mu\text{m}$ size ranged from 140–1310 particles for BAT1706 and 60–490 particles for EU-bevacizumab, for $\geq 10 \mu\text{m}$ size ranged from 10–50 particles for BAT1706 and 0–10 particles for EU-bevacizumab, and for $\geq 25 \mu\text{m}$ size 0 particles for both BAT1706 and EU-bevacizumab. US-bevacizumab was not tested for such analysis. As per Flowcam method, the cumulative particle counts per mL for $\geq 5 \mu\text{m}$ non-spherical particles ranged from 370–1301 particles for BAT1706, 505–572 particles for US-bevacizumab, and 112–1167 particles for EU-bevacizumab and for $\geq 5 \mu\text{m}$ spherical particles ranged from 90–931 particles for BAT1706, 101–158 particles for US-bevacizumab, and 23–404 particles for EU-bevacizumab. Any small differences observed were considered to be of no clinical significance.

In the DLS profile, no submicron particles were observed (Fig. 4A). Furthermore, the hydrodynamic particle size assay showed that the molecular size of BAT1706 was highly similar to that of EU/US-bevacizumab (DLS radius ranged from 7.5 to 7.6 nm for BAT1706, 7.0–7.7 nm for

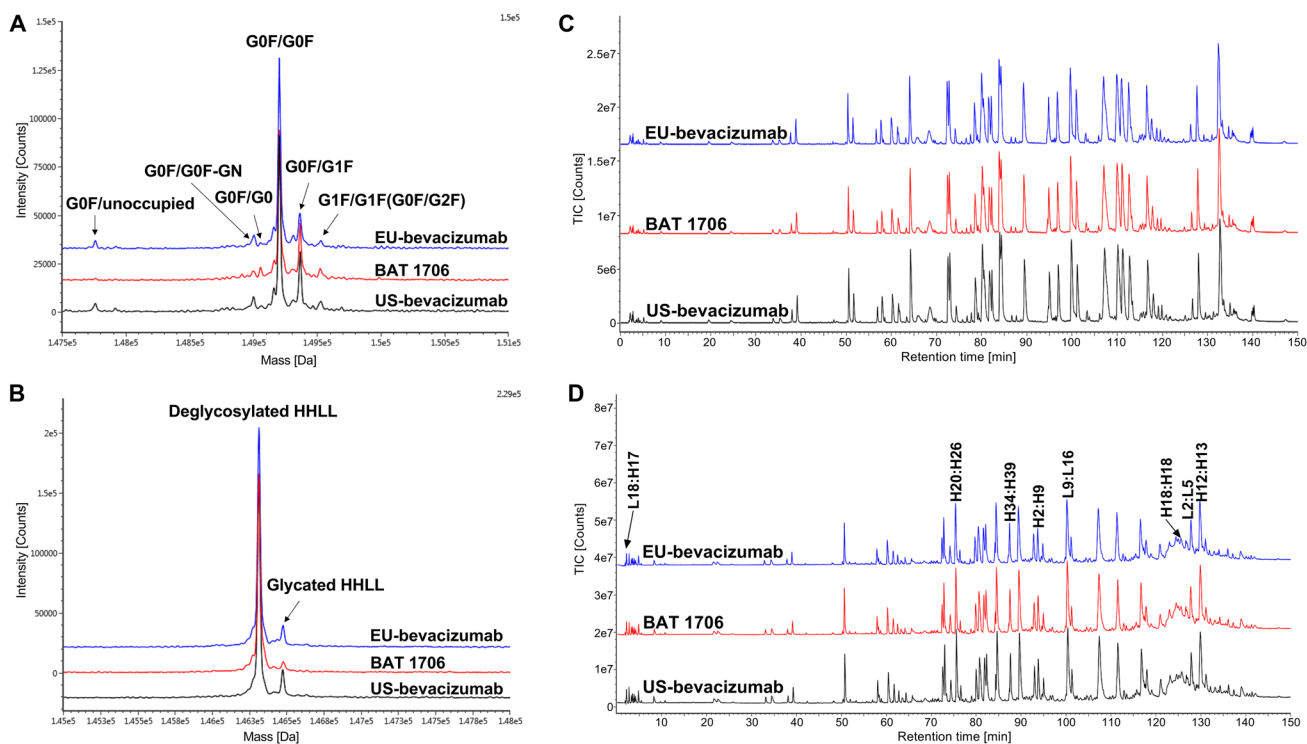
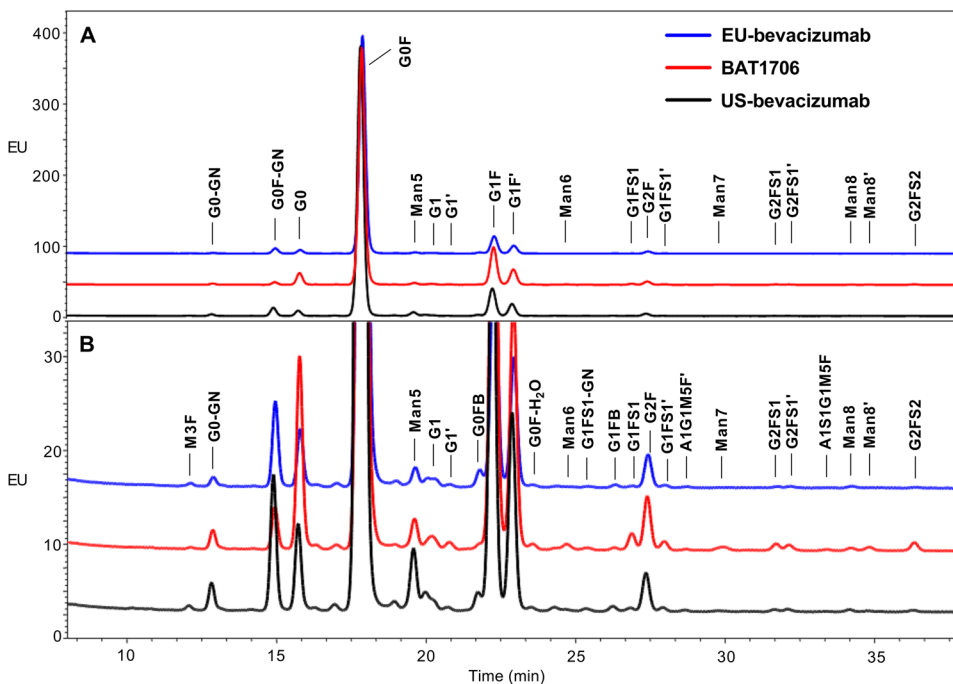


Fig. 1 Primary structure comparison of BAT1706 (Red), EU-bevacizumab (Blue) and US-bevacizumab (Black). **A** Intact molecular deconvoluted mass profile, **B** deglycosylated intact molecular decon-

voluted mass profile, **C** reduced tryptic peptide mapping, and **D** non-reduced tryptic peptide mapping.

Fig. 2 Comparison of oligosaccharide profiles of BAT1706 (Red), EU-bevacizumab (Blue) and US-bevacizumab (Black) analyzed by HILIC-UPLC. **A** Representative oligosaccharide profiles are presented for each product. The types and proportions of the glycans are conserved among the products. **B** The extensive view of each product with more detailed information. *HILIC-UPLC* hydrophilic interaction liquid chromatography-ultra-performance liquid chromatography



US-bevacizumab, and 7.3–7.5 nm for EU-bevacizumab; Table 2).

The visual comparison of the AUC profile showed that in the natural state, neither BAT1706 nor EU/US-bevacizumab had large-sized aggregates (Fig. 4B), and the levels of aggregates were similar, which correlated well with the results of the SEC-HPLC assay. Collectively, these results indicate that BAT1706 and EU/US-bevacizumab have comparable particle and aggregation levels.

3.5 Product-Related Substances and Impurities

Several techniques were applied to quantify BAT1706 and EU/US-bevacizumab product-related substances and impurities, including SEC-HPLC, IEC-HPLC, cIEF, CE-SDS, RP-HPLC, and hydrophobic interaction chromatography-high-performance liquid chromatography (HIC-HPLC). These techniques were used to quantitatively evaluate the size, charge, and hydrophobic variations.

The visual comparison showed notable similarities between the profiles of BAT1706 and EU/US-bevacizumab collected through each of these methods (Figs. 5 and 6). These results are quantified in Table 2. Results were comparable between BAT1706 and EU/US-bevacizumab, except for the level of acidic peaks (as shown by IEC-HPLC; Fig. 5B) and the level of the non-glycosylated HC peak (as shown by rCE-SDS; Fig. 5D), which were slightly lower with BAT1706. The scatter plots in Figs. 5 and 6 indicated that for SEC-HPLC, non-reduced capillary electrophoresis-sodium dodecyl sulfate (nrCE-SDS), HIC-HPLC, and RP-HPLC, more than 90% of the quantified results for BAT1706 fall in the quality range of EU/US-bevacizumab. Collectively, it can be concluded that the presence of product-related substances and impurities was highly similar between BAT1706 and EU/US-bevacizumab.

3.6 Fab-Related Biological Activities

Since binding to VEGF-A is the primary mechanism of action of bevacizumab, VEGF-A binding activity was compared between BAT1706 and EU/US-bevacizumab. VEGF-A₁₆₅ binding activity assessed by ELISA was shown to be statistically equivalent between BAT1706 and EU/US-bevacizumab (Fig. 7A, B). Specifically, the mean relative binding activity was 96% for BAT1706, 100% for US-bevacizumab, and 100% for EU-bevacizumab. The 90% confidence interval (CI) of the difference in mean binding activity between BAT1706 and US-bevacizumab (– 7.57, – 0.41%) fell

entirely within the accepted equivalence margin ($\pm 10.42\%$). Similarly, the 90% CI of the difference in mean binding activity between BAT1706 and EU-bevacizumab (– 8.05, – 0.43%) fell entirely within the accepted equivalence margin ($\pm 11.37\%$).

By using ELISA, the binding activity to other frequently expressed VEGF-A isoforms was also assessed. The results showed that BAT1706 and EU/US-bevacizumab had comparable binding activities to VEGF-A₁₂₁, VEGF-A₁₈₉ (Table 2), VEGF-A₁₄₅, and VEGF-A₂₀₆ (data not shown). For VEGF₁₂₁, the binding activity ranged from 88 to 110 for BAT1706, 85–114 for US-bevacizumab, and 85–105 for EU-bevacizumab. In the case of VEGF-A₁₈₉, the binding activity ranged from 92 to 95 for BAT1706, 94–107 for US-bevacizumab, and 89–99 for EU-bevacizumab.

Biacore™ SPR was utilized to provide a comparison of the binding kinetics of BAT1706 and EU/US-bevacizumab to VEGF-A isoforms. The on rates (k_a [association constant]), off rates (k_d [dissociation constant]), and equilibrium constant (K_D) for VEGF-A₁₂₁, VEGF-A₁₆₅ (Table 2), and VEGF-A₁₁₁ (data not shown here) binding to three different batches of BAT1706 and EU/US-bevacizumab were similar. Together, these results demonstrated that BAT1706 and EU/US-bevacizumab are highly similar in terms of binding activity to multiple isoforms of VEGF-A.

By assessing the suppression of VEGF-induced proliferation in HUVEC, a reliable indicator of VEGF-A activity *in vitro*, the biological activity of BAT1706 was compared to that of EU/US-bevacizumab.

BAT1706 and both EU/US-bevacizumab were proven to have statistically similar VEGF-A neutralizing activity (Fig. 7C, D). Specifically, the mean relative biological activity was 97% for BAT1706, 94% for US-bevacizumab, and 94% for EU-bevacizumab. The 90% CI of the difference in mean neutralizing activity between BAT1706 and US-bevacizumab (– 2.94, 8.14%) fell entirely within the accepted equivalence margin ($\pm 13.62\%$). Similarly, the 90% CI of the difference in mean neutralizing activity between BAT1706 and EU-bevacizumab (– 2.89, 7.27%) fell entirely within the accepted equivalence margin ($\pm 11.29\%$).

A reporter gene assay (RGA) has been developed to evaluate the neutralization activity of BAT1706 against VEGF-A₁₆₅. This assay is based on the VEGF-A-KDR-NFAT signaling pathway, which is regarded as one of the key angiogenesis regulatory pathways. Using this RGA assay, VEGF-A neutralizing activity was also shown to be statistically equivalent between BAT1706 and EU/US-bevacizumab (Fig. 7E, F). Specifically, the mean relative

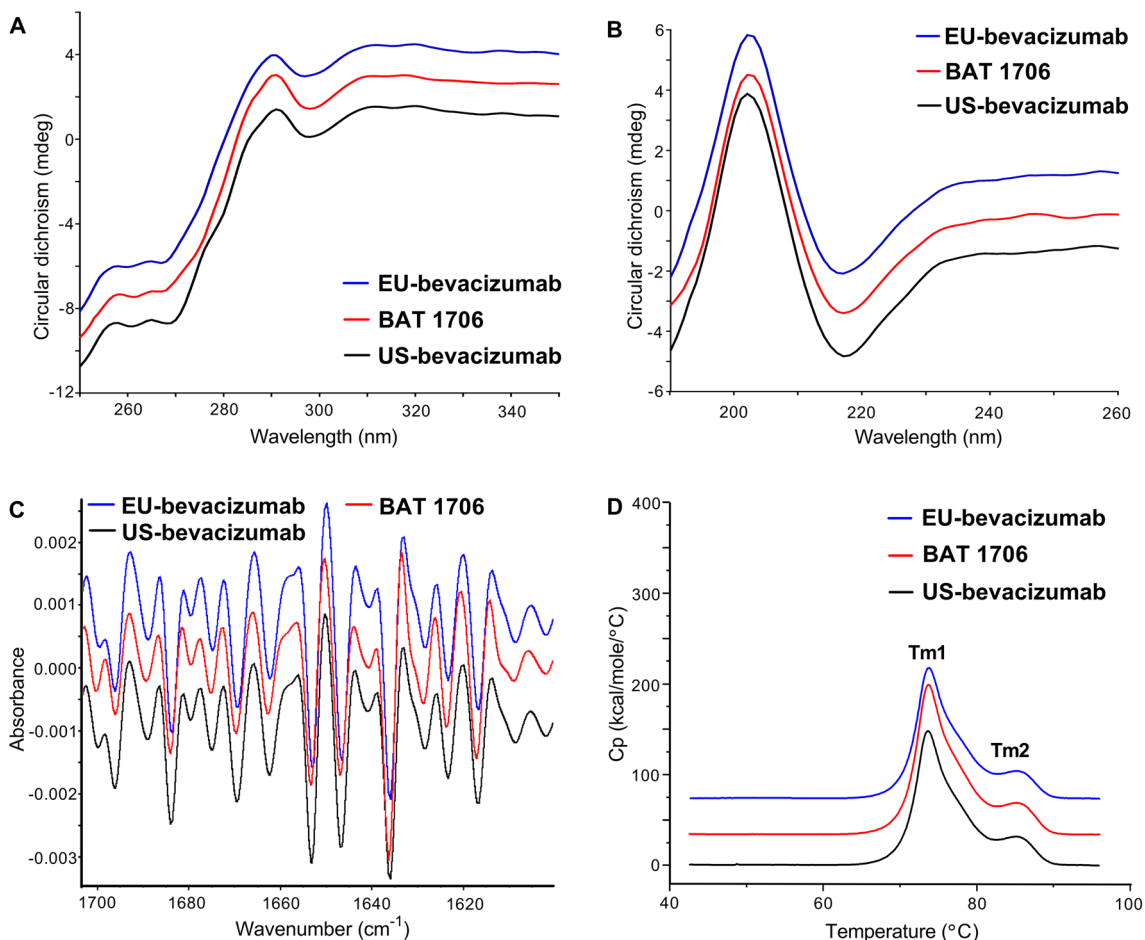


Fig. 3 Higher order structure comparison of BAT1706 (Red), EU-bevacizumab (Blue), and US-bevacizumab (Black). **A** Far-ultraviolet circular dichroism spectra, **B** near-ultraviolet circular dichroism spectra, **C** Fourier-transform infrared spectra, and **D** differential scanning calorimetry thermograms

tra, **C** Fourier-transform infrared spectra, and **D** differential scanning calorimetry thermograms

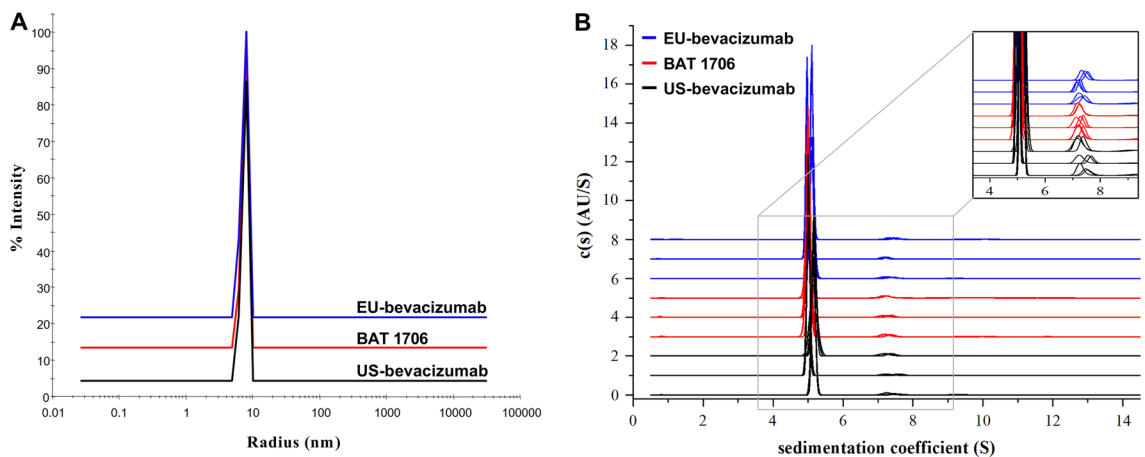


Fig. 4 Particles and aggregates comparison of BAT1706 (Red), EU-bevacizumab (Blue), and US-bevacizumab (Black). **A** Submicron particle profiles by dynamic light scattering, **B** analytical ultracentrifugation-sedimentation velocity.

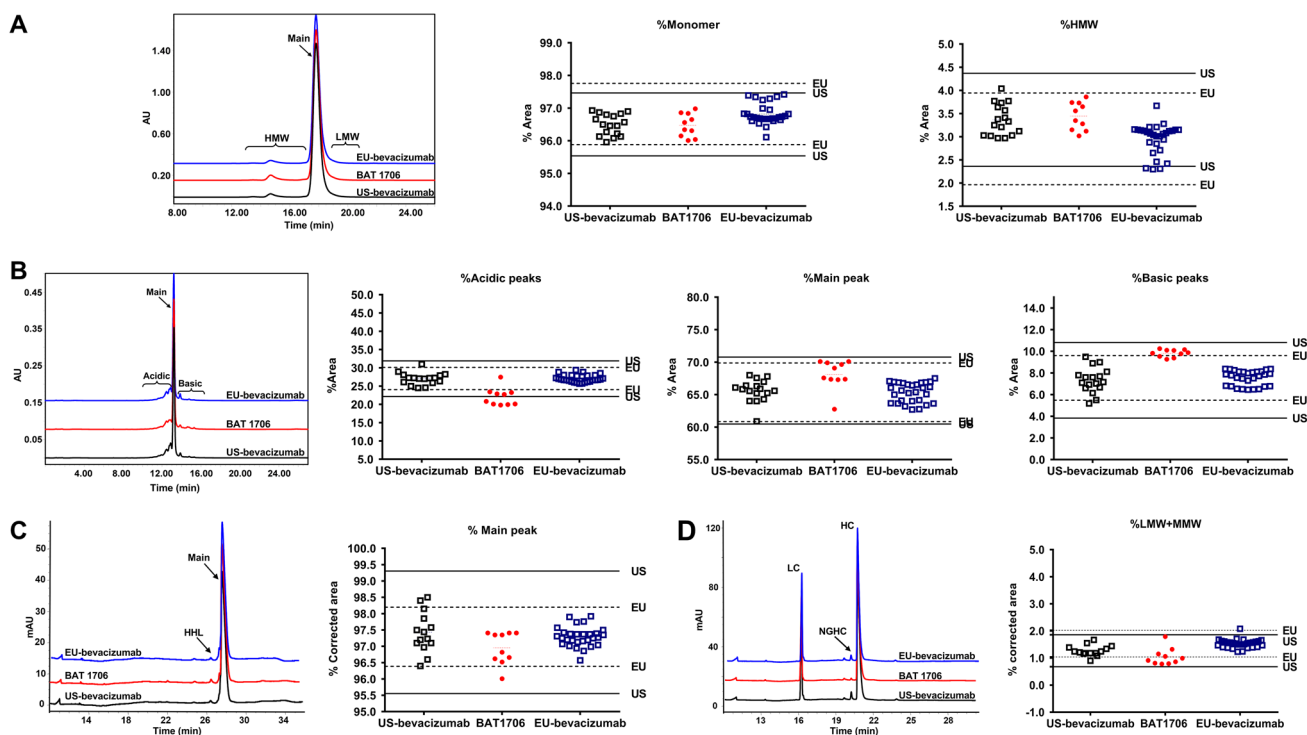


Fig. 5 Comparative physicochemical properties of size and charge variants, as assessed by **A** SEC-HPLC, **B** IEC-HPLC, **C** nrCE-SDS, and **D** rCE-SDS for BAT1706 (Red), EU-bevacizumab (Blue), and US-bevacizumab (Black). The overall profile and scatter plot distributions of different attributes are shown. IEC-HPLC cation exchange

high-performance liquid chromatography, *nrCE-SDS* non-reduced capillary electrophoresis-sodium dodecyl sulfate, *rCE-SDS* reduced capillary electrophoresis-sodium dodecyl sulfate, *SEC-HPLC* size exclusion high-performance liquid chromatography

biological activity was 95% for BAT1706, 97% for US-bevacizumab, and 94% for EU-bevacizumab. The 90% CI of the difference in mean neutralizing activity between BAT1706 and US-bevacizumab ($-5.56, 6.94\%$) fell entirely within the accepted equivalence margin ($\pm 15.93\%$). Similarly, the 90% CI of the difference in mean neutralizing activity between BAT1706 and EU-bevacizumab ($-8.36, 3.66\%$) fell entirely within the accepted equivalence margin ($\pm 17.28\%$).

The binding of VEGF-A to the VEGFR-2 expressed on endothelial cells causes the rapid autophosphorylation of the intracellular tyrosine residues of the VEGFR-2 receptor tyrosine kinase (RTK). The autophosphorylation of VEGFR-2 triggers downstream signaling cascades that result in cell proliferation and angiogenesis. The ability of BAT1706 and EU/US-bevacizumab to inhibit VEGFR-2 RTK autophosphorylation was evaluated in HUVEC. The results showed a similar dose-dependent decrease in the amount of VEGFR-2 phosphorylation across all three products. The range of EC_{50} for BAT1706, US-bevacizumab, and EU-bevacizumab was 175-223 ng/mL, 178-227 ng/mL, and 175-229 ng/mL, respectively.

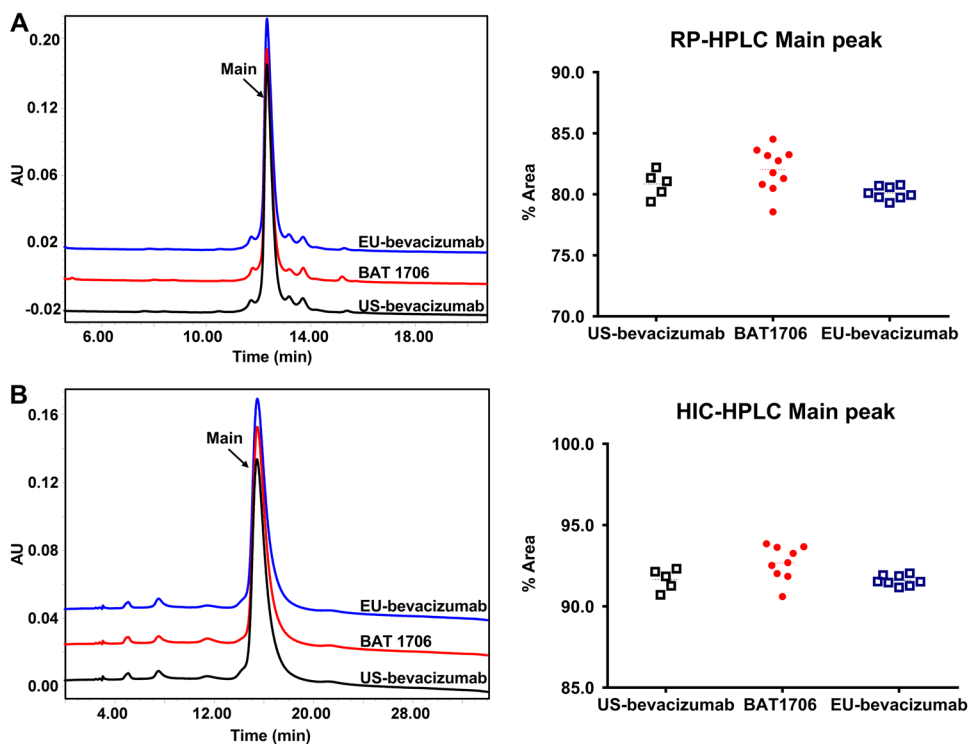
The VEGF-related ligand family consists of six members, including VEGF-A, VEGF-B, VEGF-C, VEGF-D, VEGF-E, and PLGF [15]. Bevacizumab specifically binds to VEGF-A

and blocks the biological functions of VEGF-A. The binding specificity of BAT1706 and EU/US-bevacizumab to VEGF-A was evaluated by Biacore™ SPR and was found to be VEGF-A specific (Table 2). The results showed that BAT1706 and EU/US-bevacizumab can specifically bind to VEGF-A major isoforms 165 and 121 only but fail to bind to VEGF-B, VEGF-C, VEGF-D, and PLGF [16]. The binding affinities of BAT1706 and EU/US-bevacizumab were very similar.

3.7 Fc-Related Biological Activities

The Fc region of bevacizumab binds to two distinct classes of Fc receptors: a family of Fcγ receptors (FcγR) found primarily on leukocytes, and a family of FcRn for IgG expressed primarily on endothelial cells. FcγRs contribute to immune response modulation by activation or inhibition of cellular signal transduction pathways related to inflammatory reactions or stimulation of immune effector cells. FcγRIIIa is one of the numerous FcγRs that are involved in ADCC. The determination of the half-life of serum IgG is significantly influenced by FcRn. In addition to FcγRIIIa and FcRn, other components of the immune system, such as complement, also interact with the Fc

Fig. 6 Comparative physicochemical properties of hydrophobic variants, as assessed by **A** RP-HPLC and **B** HIC-HPLC for BAT1706 (Red), EU-bevacizumab (Blue), and US-bevacizumab (Black). The right scatter plots show the data distribution for the main peak (%) in each sample by RP-HPLC (Top of right), HIC-HPLC (Top of bottom), respectively. *HIC-HPLC* hydrophobic interaction chromatography-high-performance liquid chromatography, *RP-HPLC* reverse phase-high-performance liquid chromatography



portion of bevacizumab. The mean Fc γ RIIIa binding affinities of BAT1706 and EU/US-bevacizumab evaluated by SPR were 0.769 μ M, 0.951 μ M, and 0.983 μ M, respectively. As shown in Fig. 8A, the Fc γ RIIIa binding affinities of all BAT1706 batches were within the predetermined similarity range of EU/US-bevacizumab. In this analysis, BAT1706 showed FcRn binding activity within the predetermined similarity range of EU/US-bevacizumab (Fig. 8B). In addition, Fig. 8C, D show the representative dose dependent sensorgrams of Fc γ RIIIa and FcRn, respectively, and the graphs indicate that BAT1706 also has a similar process of association and dissociation to the reference product. Fc γ RIIIa and FcRn binding activities for BAT1706 and EU/US-bevacizumab were also assessed across three tumor cell lines *in vitro*. The bioluminescent cell-based reporter gene assay revealed that BAT1706 and EU/US-bevacizumab failed to induce ADCC activity in the two VEGF-A secreting cell lines (DLD-1 and Calu-6) as well as the SKOV-3 cells, which expressed both secreted and cell-surface associated VEGF-A isoforms. These results are consistent with published literature [17]. The C1q binding activity of BAT1706 was similar to that observed for EU/US-bevacizumab. However, results from the CDC assay also showed that BAT1706 and EU/US-bevacizumab failed to induce CDC activity in the same three cell lines used in the ADCC assay, which is also consistent with published literature [17]. Binding activities to other Fc γ Rs, such as Fc γ RIa, Fc γ RIIa, Fc γ RIIb,

and Fc γ RIIIb, were also comparable between BAT1706 and EU/US-bevacizumab.

3.8 Stability and Degradation at Accelerated/Stressed Conditions

Multiple thermal stability and degradation experiments were carried out under different conditions to assess the degradation pathway and degradation rate of BAT1706 and EU/US-bevacizumab. The conditions included temperatures of 25 $^{\circ}$ C, 40 $^{\circ}$ C, and 50 $^{\circ}$ C, low pH, light exposure, oxidation, vibration, and freeze-thaw cycles.

Stability was assessed using SEC-HPLC, rCE-SDS, IEC-HPLC, and PTM methods. Degradation profiles after incubation at 50 $^{\circ}$ C for 14 days were comparable for BAT1706 and EU/US-bevacizumab, as illustrated by SEC-HPLC (Fig. 9A) and IEC-HPLC (Fig. 9B). The similarity was further demonstrated by plotting degradation rates for BAT1706 and EU/US-bevacizumab, as shown for SEC-HPLC monomer percentage (Fig. 9C), slope of EU-Bevacizumab, BAT1706 and US-Bevacizumab are -0.9668, -0.9763, -0.9017) and IEC-HPLC main peak percentage (Fig. 9D, slope of EU-Bevacizumab, BAT1706 and US-Bevacizumab are -2.925, -2.808, -2.889). The degradation rates for BAT1706 and EU/US-bevacizumab were found to be similar under all conditions for all evaluated product-related variants and potencies (not presented here).

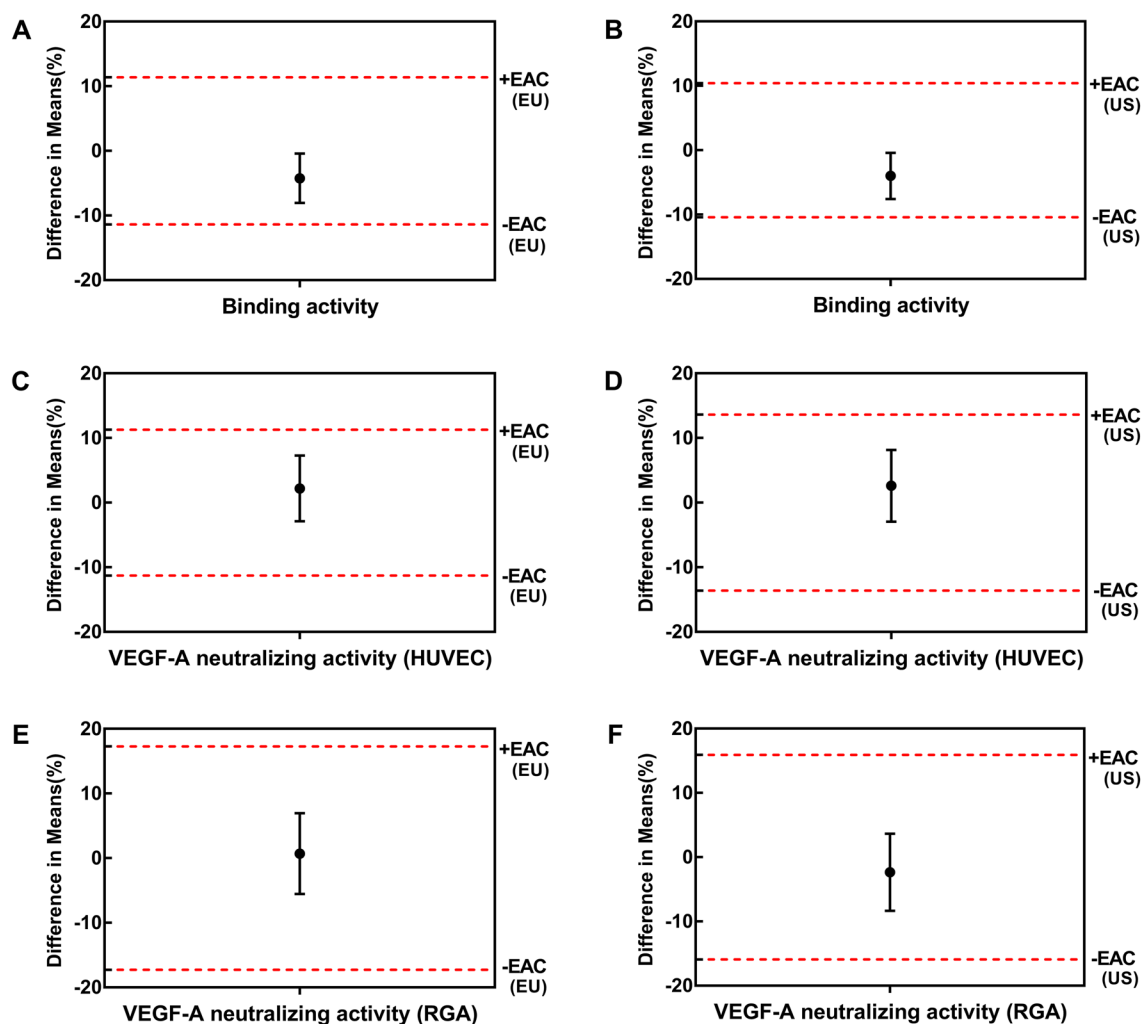


Fig. 7 Similarity analysis of the VEGF-A binding activity and neutralizing activity of BAT1706 and EU/US-bevacizumab. Equivalence testing graphs of: **A** VEGF-A₁₆₅ binding activity of BAT1706 and EU-bevacizumab by ELISA, **B** VEGF-A₁₆₅ binding activity of BAT1706 and US-bevacizumab by ELISA, **C** VEGF-A neutralizing activity of BAT1706 and EU-bevacizumab by HUVEC cell-based assay, **D** VEGF-A neutralizing activity for BAT1706 and US-bevacizumab by HUVEC cell-based assay, **E** VEGF-A neutralizing activ-

ity for BAT1706 and EU-bevacizumab by reporter gene assay, and **F** VEGF-A neutralizing activity for BAT1706 and US-bevacizumab by reporter gene assay. The graph shows the mean difference in activity between BAT1706 and EU/US-bevacizumab; error bars represent the 90% CI. The dashed lines represent the equivalence acceptance criterion (EAC). *CI* confidence interval, *ELISA* enzyme-linked immunosorbent assay, *HUVEC* human umbilical vein endothelial cells, *VEGF-A* vascular endothelial growth factor A

3.9 General Properties

As directed by regulatory authorities, it is necessary to certify that the "strength" of a biosimilar matches that of the reference medicine [18]. Analytical similarity assessments of BAT1706 and EU/US-bevacizumab strengths were performed by protein concentration and volume measurements and were found to be similar (Table 2). The protein concentration levels ranged from 24.2 to 26.6 mg/mL, 23.4 to 25.2 mg/mL, and 23.7 to 25.4 mg/mL for BAT1706, US-bevacizumab, and EU-bevacizumab, respectively. As for the

volume measurements, these levels were measured using two different volumes, 100 mg/4 mL and 400 mg/ 16 mL. In the case of 100 mg/4 mL, the levels ranged from 4.1 to 4.2 mL for BAT1706 and 4.4–4.5 mL for EU-bevacizumab, while US-bevacizumab batches were not tested. Moreover, in the case of 400 mg/16 mL, BAT1706 ranged from 16.3 to 16.8 mL, while US- and EU-bevacizumab batches were not tested. The general properties of BAT1706 and EU/US-bevacizumab, including osmolarity, pH, appearance, color, and transparency, were also compared, with all the results meeting the predetermined criteria for similarity.

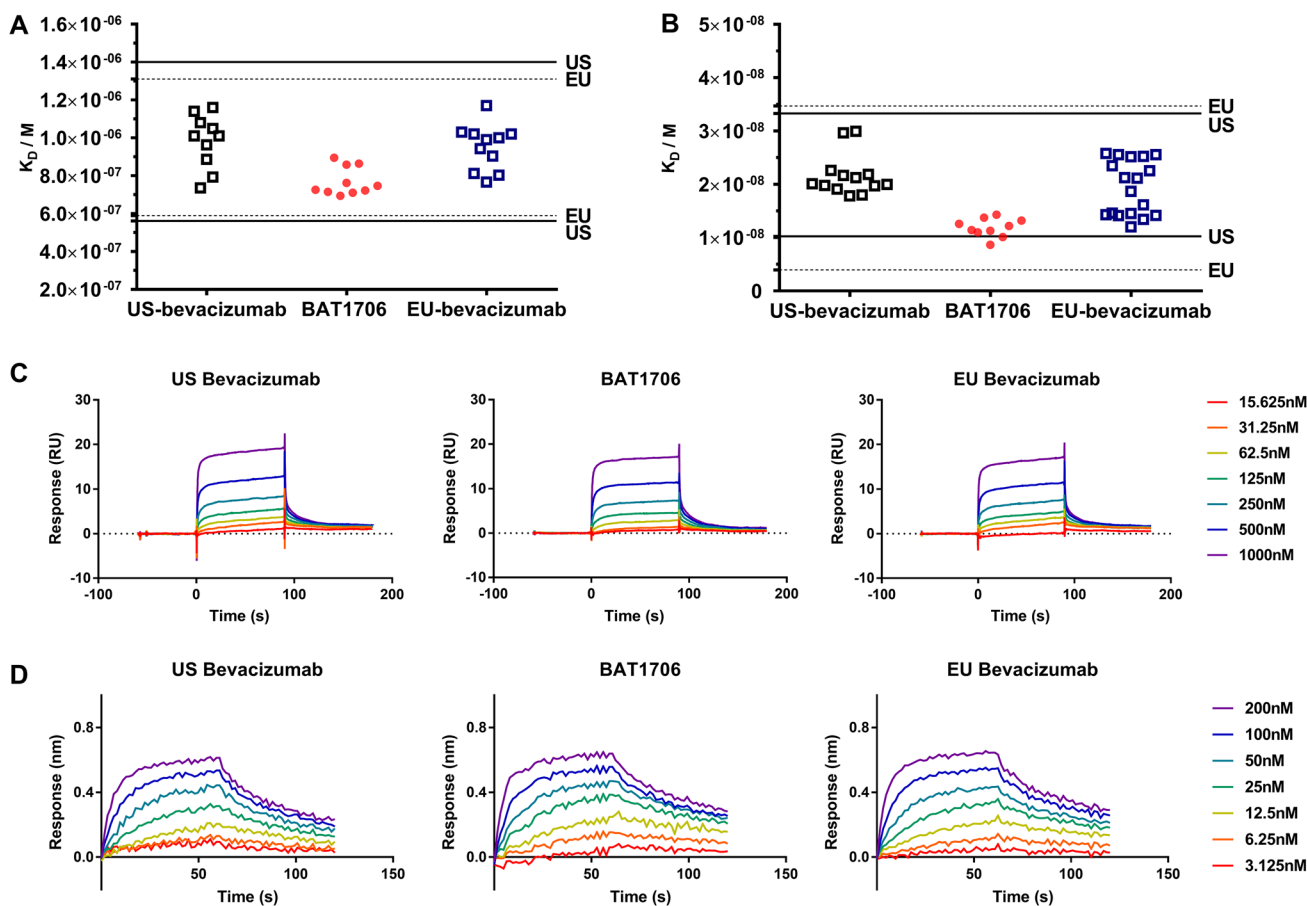


Fig. 8 Fc γ RIIIa-F158 and FcRn binding affinity assessment. **A** Scatter plot distribution of the Fc γ RIIIa-F158 binding equilibrium dissociation constant for BAT1706 and EU/US-bevacizumab. **B** Scatter plot distribution of the FcRn binding equilibrium dissociation constant for BAT1706 and EU/US-bevacizumab. **C** Corresponding dose

dependent sensorgrams of the Fc γ RIIIa-F158 binding equilibrium dissociation constant for BAT1706 and EU/US-bevacizumab for scatter plot (**A**). **D** Corresponding dose dependent sensorgrams of the FcRn binding equilibrium dissociation constant for BAT1706 and EU/US-bevacizumab for scatter plot (**B**)

3.10 Host-Cell Impurities

Considerable differences in process-related impurities between biosimilars and reference medicines may adversely affect safety. Residual host cell proteins (HCPs) in BAT1706 and EU/US-bevacizumab were quantified and characterized by orthogonal methods. Results from an HCP ELISA, using an assay specific to the BAT1706 cell line and manufacturing process, revealed low levels of HCPs for BAT1706 and EU/US-bevacizumab. While the levels of HCPs in BAT1706 (10–20 ppm) were relatively higher than the levels observed in EU/US-bevacizumab (0.2–0.9 ppm and 0.3–0.6 ppm; Table 2), as HCP test kits have high specificity and different sensitivity for different products, these data are provided for completeness only, and results should not be compared between the products.

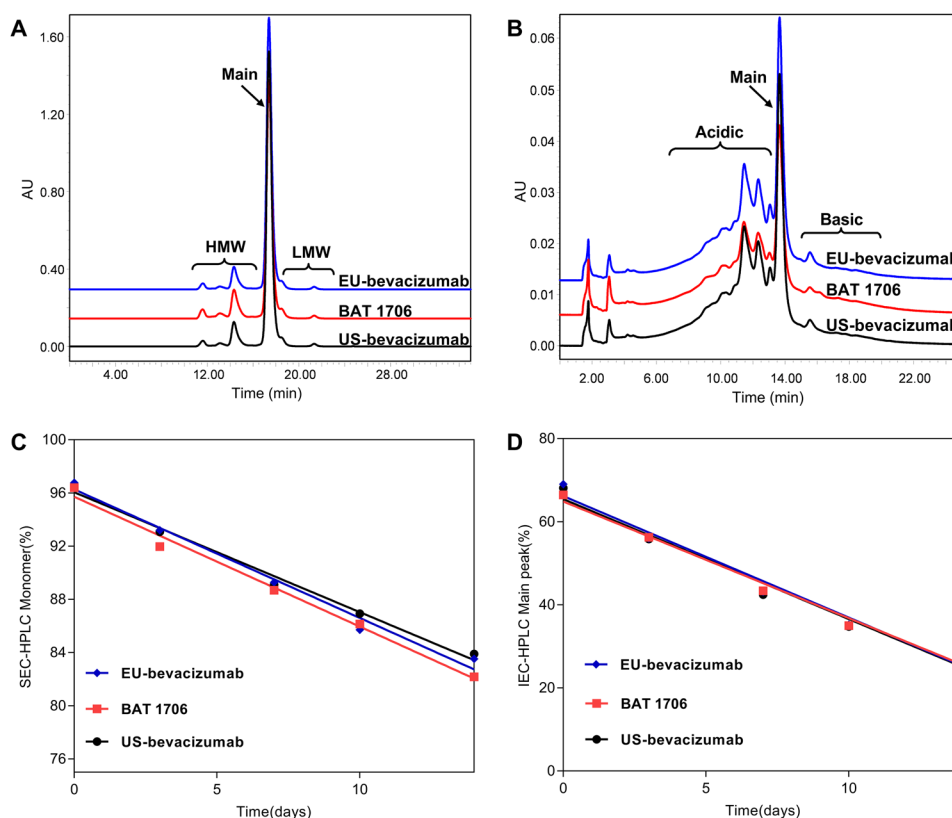
Residual protein A and DNA levels in BAT1706 and EU/US-bevacizumab were also very low or below the detection limit (data not shown here).

4 Discussion

The data from this extensive comparability exercise demonstrated that BAT1706 matches EU/US-bevacizumab in terms of all physicochemical and functional attributes assessed.

In this comparability exercise, the quality attributes were evaluated according to one of three tiers of a statistical analysis plan based on the risk ranking and other factors, using an approach recommended by the FDA [5]. Evaluation of analytical similarity between biosimilars and reference medicines can be challenging, as the availability of many of the reference and biosimilar medicines is often limited at the time of the analysis. Due to a large number of potentially heterogeneous attributes present in antibody molecules and the different nature of each attribute, there is a risk of bias if the same similarity judgment is used for all the attributes. As a result, the risk-based tier approach offers a systematic method to assess analytical similarity with a high level of confidence and less potential for bias.

Fig. 9 **A** SEC-HPLC and **B** IEC-HPLC profiles of samples incubated at 50 °C for 14 days. The degradation rate of **C** the SEC-HPLC monomer and **D** the IEC-HPLC main peak of BAT1706 (Red) and EU-bevacizumab (Blue), and US-bevacizumab (Black). *IEC-HPLC* cation exchange high-performance liquid chromatography, *SEC-HPLC* size exclusion high-performance liquid chromatography



The similarity of VEGF-A binding and neutralizing activity, the two biological activities with the highest potential clinical impact, was evaluated using an equivalence test (Tier 1). The results demonstrated that the 90% CIs of the mean difference in activity between BAT1706 and EU/US-bevacizumab were within the predefined equivalence margins. Most of the other biological activities related to Fab or Fc functions were evaluated by the quality range approach (Tier 2). Greater than 90% of the measured biological activities of all BAT1706 lots fall within the range of the quality range of EU/US-bevacizumab (Mean \pm 3SD). These results strongly support the conclusion that BAT1706 exhibits highly similar functional properties compared with reference bevacizumab.

The similarity of the physicochemical properties of BAT1706 and EU/US-bevacizumab was evaluated by quality range (Tier 2) or visual comparison (Tier 3) approaches, depending on the tier ranking of the attribute. These analyses showed BAT1706 and reference bevacizumab to have identical primary structures and indistinguishable higher-order structures, as well as highly similar purity profiles and charge isoforms.

In the Tier 2 analysis, more than 90% of the BAT1706 lots compared were within the quality range (Mean \pm 3SD) of the reference bevacizumab for most quality attributes. Minor differences in the ratio of galactosylation and afucosylation were found between BAT1706 and reference bevacizumab. However, since bevacizumab does not have ADCC and CDC

effects and the mechanism of action does not involve related effects, these minor differences are not expected to impact clinical safety and efficacy. Other minor differences observed between BAT1706 and reference bevacizumab, such as lower levels of acidic variants and higher rCE purity with BAT1706, are also not expected to impact clinical safety and efficacy. Indeed, BAT1706 has been evaluated in Phase I and III clinical studies, which have demonstrated that BAT1706 is highly similar to the reference bevacizumab in terms of clinical performance. In a Phase I trial in healthy volunteers, BAT1706 was shown to be highly similar to EU/US-bevacizumab in terms of PK equivalence (90% CI for the AUC_{0–inf} was 99–112% for BAT1706 versus EU-bevacizumab and 97–110% for BAT1706 vs US-bevacizumab), safety (no significant adverse events attributable to BAT1706, as compared to EU/US-bevacizumab), and immunogenicity (no anti-drug antibody positive result was reported for any subject) [19]. BAT1706 has also been evaluated in a Phase III trial in patients with advanced nonsquamous non-small-cell lung carcinoma, where clinical equivalence to EU-bevacizumab was demonstrated in terms of efficacy (48% patients achieving overall response rate in BAT1706 arm and 44.5% in EU-bevacizumab arm; progression-free survival at 12 months was 20.7% and 21.8%, respectively), safety (incidence of treatment-emergent adverse events [TEAEs] and study drug-related TEAEs was similar between BAT1706 and EU-bevacizumab arms), PK (mean serum

concentrations were comparable between BAT1706 and EU-bevacizumab), and immunogenicity (no positive neutralizing anti-drug antibodies in any patient) [20].

Finally, the stability of BAT1706 and EU/US-bevacizumab was assessed in a series of accelerated and forced degradation experiments. Both degradation pathways and degradation rates were shown to be similar for BAT1706 and the reference bevacizumab under all conditions evaluated. The increased acidic peaks were mainly characterized as fragments and deamidation species, as we identified from the long-term samples.

In summary, all results taken together support that the proposed bevacizumab biosimilar BAT1706 matches EU- and US-sourced reference bevacizumab in terms of all physicochemical and functional properties assessed. These findings also show that bevacizumab from the US and the EU is physicochemically and functionally comparable. The physicochemical and functional similarity between BAT1706 and the reference bevacizumab was comprehensively characterized using series state-of-the-art analytical methods, following the relevant regulatory guidelines. The similarity assessment addressed critical and relevant attributes, including the primary structure, higher-order structure, particles and aggregates, product-related substances and impurities, thermal forced degradation, biological activities, general properties, and process-related impurities for both BAT1706 and the reference bevacizumab. The results described herein contribute to the totality of evidence demonstrating biosimilarity between the proposed bevacizumab biosimilar BAT1706 and reference bevacizumab in combination with clinical study outcomes. In conclusion, the current demonstrated and positive regulatory biosimilarity review, regardless the minor differences were observed, but these differences were not clinically meaningful, therefore it can be concluded that overall product quality of BAT1706 can be considered highly similar to EU/US Bevacizumab.

Acknowledgements This study was funded by Sandoz and Bio-Thera, and this manuscript was prepared and reviewed by Sandoz. Our particular thanks go to Natalia Koptelova at Sandoz and Manca Kenig at Novartis. The authors also would like to acknowledge the entire CMC team from Bio-Thera, especially to manufacture team for sample supply support and analytical characterization technical support. Editorial support was provided by Eve Blumson of Ascend, a division of Spirit Medical Communications Group Limited.

Declarations

Funding This work was supported by the Ministry of Science and Technology of the People's Republic of China under Grant number 2013ZX09401001; Department of Science and Technology of Guangdong Province under Grant number 2013Y116.

Conflict of Interest Di Cao, Chunping Deng, Guangying Wang, Xiong Mei, Jianhua Xie, Yuanmei Liu, Yujie Liu, Yili Yang, Shengfeng Li,

and Cuihua Liu are employees and stockholders of Bio-Thera Solutions, Ltd.

Ethics This article does not contain any studies with human participants or animals. All laboratory health and safety procedures have been complied with in the course of conducting this experimental work.

Consent to participate Not applicable.

Consent for publication Not applicable.

Data Availability Data will be made available on reasonable request.

Code availability Not applicable.

Open Access This article is licensed under a Creative Commons Attribution-NonCommercial 4.0 International License, which permits any non-commercial use, sharing, adaptation, distribution and reproduction in any medium or format, as long as you give appropriate credit to the original author(s) and the source, provide a link to the Creative Commons licence, and indicate if changes were made. The images or other third party material in this article are included in the article's Creative Commons licence, unless indicated otherwise in a credit line to the material. If material is not included in the article's Creative Commons licence and your intended use is not permitted by statutory regulation or exceeds the permitted use, you will need to obtain permission directly from the copyright holder. To view a copy of this licence, visit <http://creativecommons.org/licenses/by-nc/4.0/>.

References

1. Weise M, Bielsky MC, De Smet K, Ehmann F, Ekman N, Narayanan G, Heim H-K, Heinonen E, Ho K, Thorpe R, et al. Biosimilars-why terminology matters. *Nat Biotechnol.* 2011;29(8):690–3. <https://doi.org/10.1038/nbt.1936>.
2. Beck A, Wurch T, Bailly C, Corvaia N. Strategies and challenges for the next generation of therapeutic antibodies. *Nat Rev Immunol.* 2010;10(5):345–52. <https://doi.org/10.1038/nri2747>.
3. European Medicines Agency. Guideline on similar biological medicinal products containing biotechnology-derived proteins as active substance: quality issues (revision 1). European Medicines Agency. 2014. https://www.ema.europa.eu/en/documents/scientific-guideline/guideline-similar-biological-medicinal-products-containing-biotechnology-derived-proteins-active_en-0.pdf Accessed 3 Dec 2022.
4. U.S. Department of Health and Human Services, Food and Drug Administration, Center for Drug Evaluation and Research, Center for Biologics Evaluation and Research. Development of therapeutic protein biosimilars: comparative analytical assessment and other quality-related considerations; Guidance for industry. US Food and Drug Administration. 2019. <https://www.fda.gov/media/125484/download>. Accessed 3 Dec 2022.
5. U.S. Department of Health and Human Services, Food and Drug Administration. Statistical approaches to evaluate analytical similarity; Guidance for industry. US Food and Drug Administration. 2017. <https://www.pbwt.com/content/uploads/2018/06/UCM576786.pdf>. Accessed 3 Dec 2022.
6. Ferrara N, Hillan KJ, Gerber HP, Novotny W. Discovery and development of bevacizumab, an anti-VEGF antibody for treating cancer. *Nat Rev Drug Discov.* 2004;3(5):391–400. <https://doi.org/10.1038/nrd1381>.

7. Genentech, Inc. Avastin (bevacizumab) prescribing information. Revised 2016 https://www.gene.com/download/pdf/avastin_prescribing.pdf Accessed 3 Dec 2022.
8. Goetze AM, Liu YD, Zhang Z, Shah B, Lee E, Bondarenko PV, Flynn GC. High-mannose glycans on the Fc region of therapeutic IgG antibodies increase serum clearance in humans. *Glycobiology*. 2011;21(7):949–59. <https://doi.org/10.1093/glycob/cwr027>.
9. Shields RL, Lai J, Keck R, O'Connell LY, Hong K, Meng YG, Weikert SH, Presta LG. Lack of fucose on human IgG1 N-linked oligosaccharide improves binding to human Fcγ₃ and antibody-dependent cellular toxicity. *J Biol Chem*. 2002;277(30):26733–40. <https://doi.org/10.1074/jbc.M202069200>.
10. Wang Y, Fei D, Vanderlaan M, Song A. Biological activity of bevacizumab, a humanized anti-VEGF antibody in vitro. *Angiogenesis*. 2004;7(4):335–45. <https://doi.org/10.1007/s10456-004-8272-2>.
11. Flynn GC, Chen X, Liu YD, Shah B, Zhang Z. Naturally occurring glycan forms of human immunoglobulins G1 and G2. *Mol Immunol*. 2010;47(11–12):2074–82. <https://doi.org/10.1016/j.molimm.2010.04.006>.
12. Reusch D, Tejada ML. Fc glycans of therapeutic antibodies as critical quality attributes. *Glycobiology*. 2015;25(12):1325–34. <https://doi.org/10.1093/glycob/cwv065>.
13. Hodoniczky J, Zheng YZ, James DC. Control of recombinant monoclonal antibody effector functions by Fc N-glycan remodeling in vitro. *Biotechnol Prog*. 2005;21(6):1644–52. <https://doi.org/10.1021/bp050228w>.
14. Boyd PN, Lines AC, Patel AK. The effect of the removal of sialic acid, galactose and total carbohydrate on the functional activity of Campath-1H. *Mol Immunol*. 1995;32(17–18):1311–8. [https://doi.org/10.1016/0161-5890\(95\)00118-2](https://doi.org/10.1016/0161-5890(95)00118-2).
15. Takahashi S. Vascular endothelial growth factor (VEGF), VEGF receptors and their inhibitors for antiangiogenic tumor therapy. *Biol Pharm Bull*. 2011;34(12):1785–8. <https://doi.org/10.1248/bpb.34.1785>.
16. Papadopoulos N, Martin J, Ruan Q, Rafique A, Rosconi MP, Shi E, Pyles EA, Yancopoulos GD, Stahl N, Wiegand SJ. Binding and neutralization of vascular endothelial growth factor (VEGF) and related ligands by VEGF Trap, ranibizumab and bevacizumab. *Angiogenesis*. 2012;15(2):171–85. <https://doi.org/10.1007/s10456-011-9249-6>.
17. Salvador C, Li B, Hansen R, Cramer DE, Kong M, Yan J. Yeast-derived beta-glucan augments the therapeutic efficacy mediated by anti-vascular endothelial growth factor monoclonal antibody in human carcinoma xenograft models. *Clin Cancer Res*. 2008;14(4):1239–47. <https://doi.org/10.1158/1078-0432.CCR-07-1669>.
18. U.S. Department of Health and Human Services, Food and Drug Administration. Questions and answers on biosimilar development and the BPCI act; Guidance for industry. US Food and Drug Administration. 2021. <https://www.fda.gov/media/119258/download>. Accessed 3 Dec 2022.
19. Wu X, Wynne C, Xu C, Gan Y, Wang C, Thomas BE, Yu JC, Li S, Zhang L. A global phase I clinical study comparing the safety and pharmacokinetics of proposed biosimilar BAT1706 and Bevacizumab (Avastin®) in healthy male subjects. *BioDrugs*. 2019;33(3):335–42. <https://doi.org/10.1007/s40259-019-00352-7>.
20. Chen L, Trukhin D, Kolesnik O, Rangel JDDG, Cil T, Li X, Cicin I, Kobziev O, Shen Y, Liu Z, et al. Clinical efficacy and safety of the BAT1706 (proposed bevacizumab biosimilar) compared with reference bevacizumab in patients with advanced nonsquamous NSCLC: a randomized, double-blind, phase III study. *J Clin Oncol*. 2022;40(Suppl 16):9041–9041. https://doi.org/10.1200/JCO.2022.40.16_suppl.9041.